# Neuraminidase inhibitors rewire neutrophil function in murine sepsis and COVID-19 patients' cells

Rodrigo O. Formiga[1,2], Flávia C. Amaral[1,2], Camila F. Souza[2], Daniel A. G. B. Mendes[1,2], Carlos W. S. Wanderley[3], Cristina B. Lorenzini[1,2], Adara A. Santos[1,4], Juliana Antônia[1], Lucas F. Faria[1], Caio C. Natale[1,2], Nicholas M. Paula[1,2], Priscila C. S. Silva[1], Fernanda R. Fonseca[5], Luan Aires[1,2], Nicoli Heck[1], Shana P. C. Barroso[6], Alexandre Morrot[7], Regina Sordi[2], Frederico Alisson-Silva[8], Daniel S. Mansur[1,4], Fernando Q. Cunha[3], Rosemeri Maurici[5], André Báfica[1,4], Matthew S. Macauley[9,10], Fernando Spiller[1,2*]

[1]Laboratory of Immunobiology, [2]Department of Pharmacology, [4]Department of Microbiology, Immunology and Parasitology, [5]Department of Clinical Medicine, Federal University of Santa Catarina (UFSC), Florianopolis, Santa Catarina, Brazil.
[3]Department of Pharmacology, School of Medicine of Ribeirao Preto, University of Sao Paulo, Ribeirao Preto, Sao Paulo, Brazil.
[6]Molecular Biology Laboratory, Institute of Biomedical Research, Marcilio Dias Naval Hospital, Navy of Brazil, Rio de Janeiro, Brazil.
[7]Tuberculosis Research Laboratory, Faculty of Medicine, Federal University of Rio de Janeiro, Rio de Janeiro, Brazil; Immunoparasitology Laboratory, Oswaldo Cruz Foundation, FIOCRUZ, Rio de Janeiro, Brazil.
[8]Department of Immunology, Paulo de Goes Institute of Microbiology, Federal University of Rio de Janeiro (UFRJ), Rio de Janeiro, Brazil.
[9]Department of Chemistry, [10]Department of Medical Microbiology and Immunology, University of Alberta, Edmonton, Alberta, Canada.

*Corresponding author: Fernando Spiller, Department of Pharmacology (FMC/CCB/UFSC), Av. Prof. Henrique da Silva Fontes, 321 - Trindade, Florianópolis – SC, 88040-900, Tel.: +55-48-3721-4852. e-mail: fernando.spiller@ufsc.br, spiller.farmaco@gmail.com.

**ABSTRACT**

Neutrophils overstimulation plays a crucial role in tissue damage during severe infections. Neuraminidase-mediated cleavage of surface sialic acid has been demonstrated to regulate leukocyte responses. Here, we report that antiviral neuraminidase inhibitors constrain host neuraminidase activity, surface sialic acid release, ROS production, and NETs released by microbial-activated human neutrophils. *In vivo*, treatment with Oseltamivir results in infection control and host survival in murine models of sepsis. Moreover, Oseltamivir or Zanamivir treatment of whole blood cells from severe COVID-19 patients reduces host NEU-mediated shedding of surface sialic acid and neutrophil overactivation. These findings suggest that neuraminidase inhibitors are host-directed interventions to dampen neutrophil dysfunction in severe infections.

Keywords: neuraminidase; sialic acid; sepsis; Oseltamivir; Zanamivir, neutrophil; SARS-CoV-2; COVID-19.

48 **INTRODUCTION**

49

50 Neutrophils are key components of the immune response against multiple pathogens[1].
51 However, during acute severe infections, such as sepsis and COVID-19, overactivated
52 neutrophils infiltrate vital organs and release many molecules including proteases,
53 reactive oxygen species (ROS), and neutrophil extracellular traps (NETs)[2,3]. While such
54 inflammatory mediators are essential to the control of infection, they can also damage
55 healthy cells[4]. Therefore, the function of neutrophils must be regulated to efficiently
56 clear microorganisms with minimal detrimental effects to the host.

57

58 A number of mechanisms controlling neutrophil activation have been described[5]. For
59 instance, the contents of sialic acid (Sia) have been demonstrated to regulate leukocyte
60 activation to microbial stimuli[6,7]. The dense array of Sia present in the glycocalyx of all
61 mammalian cells makes this monosaccharide a central molecule for many cellular
62 processes including: cell-cell interaction, signal transduction, and transendothelial
63 migration[8]. Neuraminidases (NEUs) are enzymes found in both pathogens and
64 mammalian hosts[9], which hydrolyze Sia residues linked to galactose, N-
65 acetylgalactosamine or polySia residues on glycoconjugates, thereby regulating many
66 physiological and pathological responses[10]. In human neutrophils, shedding of surface
67 Sia by microbial-derived NEUs leads to cellular activation, ROS production, and NETs
68 release[7,11–13]. Additionally, it has been demonstrated that LPS induces membrane-
69 associated NEU activation in murine or human macrophages and dendritic cells[14]. Upon
70 LPS binding to TLR4, NEU activity was shown to regulate NF-κB induction in

71 macrophages, suggesting a role for this enzyme during cellular activation[14].
72 Furthermore, in experimental Gram-negative sepsis or endotoxemia, NEU activity
73 mediated leukocyte dysfunction, associated with exacerbated inflammatory response
74 and high mortality rates[15,16]. As previous studies have demonstrated that pathogen-
75 derived NEU stimulate neutrophils[7,11,17], we investigated whether endogenous host
76 NEUs can be targeted to regulate neutrophil dysfunction observed in severe infections.
77
78 Here, we have identified host NEU activation as a positive regulator of microbial-
79 induced human neutrophil overactivation. Additionally, we have employed the antiviral
80 NEU inhibitors Oseltamivir and Zanamivir to explore this pathway and found that these
81 drugs fine-tune the neutrophil dysfunction observed in sepsis and COVID-19. Together,
82 our results show that NEU is a potential target for the control of neutrophil dysfunction
83 and presenting Oseltamivir or Zanamivir as adjunctive therapy for severe infections.

## RESULTS

### LPS-induced surface Sia shedding in human neutrophils is mediated by NEU activity

As activated NEUs hydrolyze Sia residues linked to underlying galactose glycoconjugates[8], we employed a flow cytometry-based lectin binding assay to measure Sia levels on neutrophils after their activation. Alpha2-3-Sia is a major functional Sia linkage of surface glycans present on human neutrophils[18]. Therefore, we used the lectin MAL-II that binds selectively to α2-3- over α2-6-linked Sia[19]. LPS treatment of whole blood from healthy donors significantly reduces the binding of MAL-II on neutrophils ($CD66b^+$) when compared to untreated cells (**Supplementary Fig. 2A**). Next, cells were stained with Fc-chimera of Siglec-9, a sialic acid-binding protein that recognize Sia in α2-3 and α2-6 linkages[20]. Similarly, we observed that binding of Siglec-9-Fc (**Supplementary Fig. 2B**) is decreased on neutrophils treated with LPS, confirming a reduction of neutrophil Sia residues likely due to LPS-induced NEU activity in these cells. To test this hypothesis, we measured NEU activity in human leukocytes using the NEU substrate 4-MU-NANA[14] and validated the assay using NEU purified from *C. perfringens* (CpNEU) (**Fig. 1A-B)**. Both clinically available NEU inhibitors Oseltamivir and Zanamivir reduce CpNEU activity (**Fig. 1A-B)**. Using total leukocytes from healthy donors, we observed that LPS-induced NEU activity was significantly inhibited by Oseltamivir or Zanamivir (**Fig. 1C-D**). Moreover, these NEU inhibitors prevent LPS- or CpNEU-mediated reduction of MAL-II binding on neutrophils surface

107 (**Fig. 1E-H**). Together, these results show that LPS-induced host NEU activity
108 decreases Sia content on neutrophils, which can be inhibited by Oseltamivir and
109 Zanamivir.
110
111 **LPS-induced phagocytosis and killing of *E. coli* is modulated by NEU activity**
112
113 Bacteria uptake and killing are important functions of neutrophils[4]. We next investigated
114 whether host NEU regulates phagocytosis and killing of *E. coli.* Whole blood or total
115 leukocytes from healthy donors were preincubated with LPS or CpNEU, respectively,
116 and *E. coli* BioParticles® added to cells for 60 min. Ingested pHrodo *E. coli* by
117 neutrophils were analyzed by flow cytometry. As expected, we observed a significant
118 increase in MFI of pHrodo *E. coli* of unstimulated cells at 37 $^{o}$C when compared to cells
119 at 4 $^{o}$C (**Supplementary Fig. 3**). LPS (**Fig. 2A-C**) or CpNEU, used as a positive control
120 (**Fig. 2D-F**), but not heat-inactivated CpNEU, significantly enhances phagocytosis of *E.*
121 *coli*. Remarkably, these effects are inhibited by Zanamivir or Oseltamivir (**Fig. 2A-F**),
122 suggesting that LPS-enhanced phagocytosis involves a host NEU-dependent pathway.
123 Similarly, pretreatment of cells with LPS or CpNEU increases both the number of cells
124 with bacteria as well as the number of bacteria per cell (**Fig. 2G-J**). These effects were
125 also abolished when NEU inhibitors Oseltamivir and Zanamivir were added in the cell
126 cultures (**Fig. 2G-J**). Furthermore, LPS or CpNEU treatment enhances intracellular and
127 extracellular killing of *E. coli,* which are also inhibited by Oseltamivir or Zanamivir (**Fig.**
128 **2K-L**). These results suggest that NEU plays a critical role in LPS-stimulated
129 phagocytosis and killing responses of neutrophils.

130

131 **NEU blockade prevents neutrophil activation**

132 Shedding of cell surface Sia by mobilization of granule-associated NEU to the cell
133 surface has been associated with neutrophil activation[21]. Therefore, we analyzed
134 surface expression of CD66b and CD62L, two markers of human neutrophil activation[22–
135 24], and α2-3-Sia levels in LPS-exposed whole blood cultures. Both Oseltamivir and
136 Zanamivir inhibit LPS-induced shedding of α2-3-Sia (**Fig. 3A,B**) and CD62L (**Fig. 3D,E**)
137 or upregulation of CD66b (**Fig. 3G,H**) on neutrophils. Similarly, MAL-II preincubation,
138 which prevents hydrolysis of α2-3-Sia by NEU[25] by steric hindrance at the NEU
139 cleavage site, blocks LPS-induced neutrophil activation (**Fig. 3C,F,I).** These data show
140 that dampening NEU activity or blocking the hydrolysis of α2-3-Sia is sufficient to inhibit
141 human neutrophil activation by LPS. Similar results were observed in soluble CpNEU-
142 treated leukocytes (**Supplementary Fig. 4**). Next, we assessed whether NEU inhibitors
143 influenced LPS-stimulated ROS production and NETs release, key mediators of
144 bacterial killing and tissue injury[26]. We observed that neutrophils primed with LPS and
145 stimulated with PMA produce higher amounts of ROS when compared to unprimed cells
146 **(Fig. 3J-L)**. Both Oseltamivir and Zanamivir inhibit ROS release to levels similar to
147 unprimed cells. These results were also reproduced by the treatment of cells with
148 CpNEU (**Supplementary Fig. 5E-G**). Furthermore, Oseltamivir or Zanamivir
149 significantly inhibit LPS-induced NETs released by isolated neutrophils **(Fig. 3M)**.
150 Together, these data indicate that microbial-induced host NEU activity regulates
151 important neutrophil functions *in vitro*.

152

153 **Oseltamivir enhances survival rate of mice in clinically relevant models of sepsis**

154 Exacerbated neutrophil responses such as increased ROS production, NETs release,
155 and degranulation are associated with tissue injury and organ dysfunction[27]. By using
156 Oseltamivir as a therapeutic tool, we next explored the involvement of NEU activity *in*
157 *vivo* during experimental sepsis, a model of neutrophil dysfunction[3,28,29]. We first
158 induced sepsis by intraperitoneal administration of 1 x $10^7$ CFU/mice of the Gram-
159 negative *E. coli* (ATCC 25922), which lacks NEU in its genome[30]. We used the dose of
160 10 mg/Kg of Oseltamivir by oral gavage (PO), which is the equivalent dose used in
161 humans (~7.5 mg/Kg)[31]. Oseltamivir pretreatment (2 hr before infection) plus post-
162 treatment (6 hr after infection, 12/12 h, PO, for 4 days) markedly boost host survival
163 (**Supplementary Fig. 6A**). Only a single dose of Oseltamivir before (2 hr) bacterial
164 administration was sufficient to reduce disease pathology. Oseltamivir significantly
165 decreases the number of neutrophils in the BAL and lung tissue 4 or 6 hr after infection
166 (**Supplementary Fig. 6B-C**). This pretreatment also augments the neutrophil migration
167 to the focus of infection, which is associated with an efficient control of infection
168 (**Supplementary Fig. 6D-F**). Furthermore, pretreatment with Oseltamivir decreases
169 BAL and plasma TNF and IL-17 levels (**Supplementary Fig. 6G-J**) and tissue injury
170 markers (AST, ALT, ALP and total bilirubin) (**Supplementary Fig. 6K-N**), as well as
171 prevents reduction of α2-3-Sia on peritoneal lavage $SSC^{high}$/GR-$1^{high}$ cells
172 (**Supplementary Fig. 6O-P**). More importantly, the post-treatment efficacy of
173 Oseltamivir was also evaluated in survival of septic mice. Mice were IP challenged
174 with *E. coli* (1 x $10^7$ CFU/mice) and treated 6 hr after infection with Oseltamivir for 4
175 days (10 mg/Kg, PO, 12/12h). Strikingly, in the post-treatment protocol, Oseltamivir

176 provides a significant improvement in the survival rate of septic mice (**Supplementary**
177 **Fig. 6Q**).
178
179 Next, we employed the CLP model to evaluate the effect of Oseltamivir in septic mice,
180 as it is considered the gold standard in preclinical sepsis[32]. Six hours after CLP, mice
181 were treated with Oseltamivir for 4 days (10 mg/Kg, PO, 12/12h). This treatment leads
182 to a small delay in the mortality rate of severe septic mice (**Fig. 4A**). Next, CLP septic
183 mice were treated with antibiotics because it is one of the standard interventions used in
184 clinical settings of sepsis[33]. Importantly, compared to the control animals, therapeutic
185 use of Oseltamivir plus antibiotics drastically improved survival rates of CLP mice
186 (87.5% experimental group vs 25% control group) (**Fig. 4B**). Forty-eight hr after surgery,
187 post-treated septic mice have a significant reduction of neutrophils in BAL and lungs,
188 improvement of neutrophil migration at the focus of infection, and reduced bacterial load
189 in PL and blood (**Fig. 4C-G**). Levels of TNF and IL-17 in PL and plasma and tissue
190 injury markers were also reduced in Oseltamivir treated mice (**Fig. 4H-O**). Additionally,
191 Oseltamivir also leads to a higher expression of α2-3-Sia on $SSC^{high}$/GR-$1^{high}$ cells in PL
192 (**Fig. 4P-Q**) confirming blockade of NEU activity *in vivo*.
193
194 As respiratory tract infections, particularly pneumonia, are among the most common
195 sites of infection in sepsis[34], we intratracheally administered *K. pneumoniae* (ATCC
196 700603) into mice to address the effect of Oseltamivir. Post-treatment of mice with
197 Oseltamivir significantly improves survival of septic mice challenged with *K.*
198 *pneumoniae* (**Fig. 5A**). The increased host survival was accompanied by a decrease of

199 neutrophil migration in BAL, reduced levels of TNF and IL-17 and reduced levels of
200 tissue injury markers (**Fig. 5B-K**). Oseltamivir also prevents reduction of α2-3-Sia on
201 BAL SSC$^{high}$/GR-1$^{high}$ cells (**Fig. 5L-M**). Together, these results show that host NEU
202 activation exacerbates inflammatory responses during sepsis and the use of Oseltamivir
203 improves disease outcome.
204
205 **Oseltamivir and Zanamivir rescue overactivated neutrophils from COVID-19**
206 **patients**
207
208 Similar to bacterial sepsis, recent evidence suggests that neutrophils fuel hyper-
209 inflammatory response during severe SARS-CoV-2 infection. Larger numbers of
210 circulating neutrophils have been associated with poor prognosis of COVID-19 patients
211 and analysis of lung biopsies and autopsy specimens showed extensive neutrophil
212 infiltration[2,35–41]. For instance, using single-cell analysis of whole blood from mild and
213 severe COVID-19 patients, Schulte-Schrepping *et al*. (2020) showed that neutrophils in
214 severe patients are highly activated, mainly characterized by the shedding of CD62L[42].
215 Confirming previous findings, we observed that neutrophils from active COVID-19
216 patients, but not from convalescent patients, displayed shedding of CD62L (**Fig. 6A**)
217 and upregulation of CD66b (**Fig. 6B**), indicating a high activation state of these cells.
218 Moreover, neutrophils from severe COVID-19 patients were found to present a
219 significant reduction of surface α2-3-Sia (**Fig. 6C)**, suggesting that NEU activity is
220 increased during severe COVID-19. Therefore, we ask whether neuraminidase
221 inhibitors can rescue neutrophil activation from COVID-19 patients. *Ex vivo* treatment of

222 whole blood with Oseltamivir or Zanamivir decreased neutrophil activation and restored
223 the levels of cell surface α2-3-Sia (**Fig. 6D-F**). **Fig. 6G** summarizes the effects of
224 Oseltamivir and Zanamivir on the surface levels of CD62L and α2-3-Sia by neutrophils,
225 where these treatments lead to a formation of two different clusters in cells from severe
226 COVID-19 patients. As soluble NEU enzymes are also present in plasma[15], we next
227 asked if plasma from COVID-19 patients can induce neutrophil response from healthy
228 donors. Indeed, stimulation of whole blood from healthy donors with fresh plasma from
229 severe, but not convalescent, COVID-19 patients leads to neutrophil activation (**Fig.**
230 **6H**), reduction of α2-3-Sia (**Fig. 6I**) as well as ROS production (**Fig. 6J,K**), which were
231 significantly reduced by Oseltamivir or Zanamivir (**Fig. 6H-J**). Additionally, we observed
232 that activity of NEU is increased in plasma from severe COVID-19 patients
233 (**Supplementary Fig. 7A)**. Serum glycoproteins from severe COVID-19 patients also
234 presented reduced levels of α2-3-Sia (**Supplementary Fig. 7B-E**) suggesting NEU
235 activation *in vivo*. Moreover, plasma samples from severe COVID-19 patients that were
236 heat-inactivated to inhibit soluble NEU activity **(Supplementary Fig. 7F**) still induces
237 neutrophil activation, suggesting that cellular NEU in conjunction with circulating factors
238 mediate NEU-dependent neutrophil activation in severe COVID-19. These results
239 highlight host NEU as a regulator of neutrophil activation in severe COVID-19 and
240 suggest this pathway as a potential host-directed intervention target to rewire neutrophil
241 responses during severe disease.

242 **DISCUSSION**

243

244 Systemic inflammatory response may lead to unsuitable neutrophil stimulation, which is
245 associated with higher mortality rates in sepsis and sepsis-like diseases[43]. Therefore,
246 finding new therapeutic options to prevent neutrophil overstimulation while maintaining
247 their microbicidal abilities is hugely desired. Neuraminidase inhibitors are promising
248 drugs to fill this gap. Here we demonstrated that endogenous host NEUs mediate
249 exacerbated inflammatory responses by primary neutrophils. Clinically used viral NEU
250 inhibitors, Oseltamivir and Zanamivir, decrease human NEU activity and are effective in
251 prevent LPS-induced neutrophil responses or to rescue overactivation of neutrophils
252 from COVID-19 patients. In severe murine sepsis, therapeutic use of Oseltamivir fine-
253 tunes neutrophil migration results in bacterial clearance and high survival rates.

254

255 All of the four different isotypes of NEU described in mammals (NEU1, NEU2, NEU3
256 and NEU4) remove Sia from glycoproteins and glycolipids with specific substrate
257 preferences[44]. NEU1 cleaves preferentially α2-3-Sia and seems to be the most
258 important isoenzyme in immune cells. NEU1 is a lysosomal enzyme but it is also
259 present at the cell surface where it can regulate multiple receptors such as Fc gamma
260 receptor (FcγR), insulin receptor, integrin β-4, and TLRs[45]. While several stimuli were
261 described to induce NEU activity including LPS[14], PMA, calcium ionophore A23187,
262 fMLP[21], and IL-8[46], how NEUs are activated is poorly understood. However, NEU1
263 activation involves formation of a multicomplex of enzymes that stabilizes NEU1 in its
264 conformational active state[47]. Interestingly, NEU1 was found to be associated with

265 matrix metalloproteinase-9 (MMP9) at the surface of naive macrophages[48]. LPS binding
266 to TLR4 leads to activation of a G protein-coupled receptor (GPCR) via Gαi subunit and
267 MMP9 to induce NEU1 activity, which in turn removes α2-3-Sia from TLR4, allowing its
268 dimerization and intracellular signaling[25,48,49]. Although we have not formally addressed
269 whether the LPS-TLR4 pathway directly activates NEU function in human neutrophils,
270 our results employing MAL-II preincubation suggest desialylation is required for LPS-
271 mediated neutrophil responses. Thus, it is possible that NEU controls Sia levels in TLR4
272 molecules in human neutrophils as observed in macrophages and dendritic cells[25,49].
273 The effects of LPS on neutrophil responses observed here are in accordance with the
274 well-documented induction of ROS and NETs as well as in phagocytosis and bacterial
275 killing by these phagocytes[50–54]. Importantly, the upstream involvement of NEU
276 regulating LPS responses by neutrophils is in agreement with the previous
277 demonstration that TLRs stimulate these cells independent of gene transcription[50].
278 Together, our data suggests that NEU activation provides a fast response to enhance
279 microbial-induced neutrophil functions. Thus, we speculate that this could be an
280 evolutionary mechanism by which neutrophils quickly mobilize their microbicidal
281 mediators against pathogens.
282
283 Sialic acid removal from neutrophils surface markedly changes their adhesiveness,
284 chemotaxis, and migration[21,55–58]. In peritonitis- or pneumonia-induced sepsis in mice,
285 we observed that Oseltamivir prevented the massive neutrophil infiltration into
286 bronchoalveolar spaces or lung tissues, suggesting that regulation of neutrophil
287 migration by dampening NEU activity contributes to survival of septic mice. Interestingly,

288 we observed a divergent effect of Oseltamivir on neutrophil migration to the focus of
289 infection between peritonitis- and pneumonia-induced sepsis. This could be explained
290 by the different mechanisms involved in neutrophil migration to the peritoneal cavity and
291 lungs. While expression of CD62L and rolling of neutrophils to endothelium is necessary
292 for its migration to the peritoneal cavity, it seems to be not required for migration into the
293 lungs[3,59]. Moreover, systemic neutrophil activation leads to cell stiffening, resulting in
294 retention of neutrophils in the small capillaries of the lungs[60], which is frequently the first
295 organ impaired in non-pneumonia- and pneumonia-induced sepsis[61]. The role of NEU-
296 induced neutrophil activation suggested here is in agreement with previous
297 demonstration that NEU1 deletion in hematopoietic cells confers resistance to
298 endotoxemia[16]. Also, the sialidase inhibitor Neu5Gc2en protects endotoxemic irradiated
299 wild-type (WT) mice reconstituted with WT bone marrow but not WT mice reconstituted
300 with NEU1$^{-/-}$ bone marrow cells[16]. Similar to our finds, the treatment of mice with NEU
301 inhibitors increases host survival in *E. coli*-induced sepsis[15]. This outcome was
302 correlated with significant inhibition of blood NEU activity. Enhancement of soluble NEU
303 activity in serum decreases the Sia residues from alkaline phosphatase (APL) enzymes,
304 which are involved in the clearance of circulating LPS-phosphate during sepsis[15].
305
306 SARS-CoV-2 infection leads to mild illness in most of the patients, but ~20% of them
307 progress to severe disease with many characteristics resembling sepsis, including acute
308 respiratory distress syndrome (ARDS), cytokine storm, and neutrophil dysregulation[38,62–
309 64]. The transcriptional programs found in neutrophil subsets from blood and lungs of
310 severe, but not mild, COVID-19 patients are related to cell dysfunction, coagulation, and

311 NETs formation[39,42]. We observed that blood neutrophils from severe COVID-19 are
312 highly activated as demonstrated by reduced CD62L expression and increase of CD66b
313 expression, as previously reported[42]. We now add new information by showing that
314 neutrophils from severe, but not convalescent, COVID-19 patients have reduced
315 surface levels of α2-3-Sia, suggesting a relevant role of NEU for neutrophil activation
316 during COVID-19. More importantly, both the NEU inhibitors Oseltamivir and Zanamivir,
317 increased the α2-3-Sia content and rewired the overactivation of neutrophils from
318 severe COVID-19 patients. We speculate that the addition of NEUs competitive
319 inhibitors allowed the endogenous sialyltransferases to restore sialyl residues on
320 surface glycoconjugates. Fast changes of surface sialic acid levels by sialidases and
321 sialyltransferases seems to be an important mechanism to control neutrophil
322 response[55]. In neutrophils from healthy donors or COVID-19 convalescent patients,
323 Oseltamivir and Zanamivir did not interfere in resting state and had no effect on α2-3-
324 Sia content, suggesting that NEU has a low effect on surface Sia turnover on non-
325 activated neutrophils. How neutrophils are activated and the role of NEU in this process
326 remains to be defined in COVID-19, nevertheless, recent evidence showed that
327 neutrophils could be directly activated by SARS-CoV-2[2], cytokines[65], and alarmins[39,42]
328 such as calprotectin[39], a TLR4 ligand[66]. In addition, we now add new evidence by
329 showing that soluble NEU together with other circulating factors present in plasma from
330 severe COVID-19 patients also accounts for neutrophil activation.
331
332 Collectively, this work suggests that host NEU activation leads to shedding of surface
333 sialic acid with consequent neutrophil overstimulation, tissue damage, and high

334 mortality rates. On the other hand, NEU inhibitors-prevented shedding of sialic acid and
335 regulates neutrophil response, resulting in infection control and high survival rates
336 (working model in **Supplementary Fig. 8**). Taking into account that both drugs are
337 broadly used in humans with well-known toxic and adverse effects, our data suggest
338 Oseltamivir and Zanamivir could be repurposed for the treatment of sepsis or severe
339 infections such as COVID-19. Interestingly, a retrospective single-center cohort study
340 including 1190 patients with COVID-19 in Wuhan, China, showed that administration of
341 Oseltamivir was associated with a decreased risk of death in severe patients[67]. Our data
342 suggest that such encouraging results may be explained by the inhibition of NEU-
343 mediated neutrophil dysfunction *in vivo*. Nevertheless, randomized clinical trials with
344 clinically used NEU inhibitors in sepsis and COVID-19 are required to directly explore
345 this hypothesis.

346 **MATERIALS AND METHODS**

347

348 **Human blood samples**

349 Blood was collected from healthy donors (25 - 45 yr old, n=3-12) in endotoxin-free tubes
350 with $K_3EDTA$ (Labor Import, Brasil). All participants gave their written informed consent
351 for blood collection after been informed on procedures. The research protocol followed
352 the World Medical Association Declaration of Helsinki and was approved by the
353 Institutional Review Board of the Federal University of Santa Catarina (CAAE
354 #82815718.2.0000.0121). Blood samples were also collected from severe COVID-19
355 (n=6) or convalescent COVID-19 (n=8) patients (25 to 89 yr old) admitted in the
356 Intensive Care Unit (ICU) or NUPAIVA (Research Center on Asthma and Airway
357 Inflammation) at the UFSC University Hospital from August to October 2020. Blood
358 samples from sex-matched healthy donors were used as controls. All patients or a close
359 family member gave consent for participation in the study, which was approved by the
360 UFSC IRB (CAAE #36944620.5.1001.0121). Supplementary Table 1 summarizes
361 patients clinical and laboratory records. These samples were used to analyze neutrophil
362 activation, surface α2-3-Sia as well as the effect of plasma under these parameters and
363 ROS production. Blood samples were also collected from severe COVID-19 (n=5)
364 patients (55 to 73 yr old) admitted at the Hospital Naval Marcílio Dias (HNMD). The
365 research was approved by the Research Ethics Committee (CEP) from Brazilian
366 National Health Council. All patients signed a free and informed consent form following
367 current legislation and the relevant ethical regulations approved by the Hospital Naval
368 Marcílio Dias (CAAE #31642720.5.0000.5256). These samples were used to analyze

369 the sialylation of plasma proteins. Supplementary Table 2 summarizes the clinical and
370 laboratory information of patients from this cohort.
371
372 **Evaluation of neutrophil activation, phagocytosis, killing, ROS, and NETs release**
373 Whole blood containing 1 x $10^6$ leukocytes were incubated (37 $^oC$, 5% $CO_2$) in the
374 presence or absence of Oseltamivir (100 µM, Sigma-Aldrich, San Luis, MO, USA),
375 Zanamivir (30 µM, Sigma-Aldrich), LPS (1 µg/mL, *E. coli* 0127:b8, Sigma-Aldrich), LPS
376 plus Oseltamivir or LPS plus Zanamivir for 90 min. Concentrations of Oseltamivir and
377 Zanamivir used here were chosen by concentration-effect experiments (10-100 µM
378 Oseltavimir and 1-30 µM Zanamivir) (data not shown). Since plasma is a rich source of
379 glycoconjugates, total leukocytes were used instead of whole blood to evaluate the
380 effect of isolated neuraminidase from *Clostridium perfringens* (CpNEU) on neutrophils.
381 Red blood cells (RBCs) were lysed by lysis buffer (0.15 M $NH_4Cl$; 0.1 mM EDTA; 12 mM
382 $Na_2HCO_3$) for 7 min, RT, followed by centrifugation (270 x g; 22°C; 7 min). Total
383 leukocytes (1 x $10^6$ cells) were incubated (37 $^oC$, 5% $CO_2$) in the presence or absence
384 of CpNEU (10 mU, Sigma-Aldrich), CpNEU plus Oseltamivir (100 µM) or CpNEU plus
385 Zanamivir (30 µM) for 60 min. Next, the following assays were performed. *Analysis of*
386 *neutrophil activation*. Leukocytes were then washed and resuspended in FACS buffer (2
387 mM EDTA/PBS). The mix of antibodies against CD66b (G10F5; BioLegend, San Diego,
388 CA, USA), CD62L (DREG-56; BioLegend), CD16 (3G8; BioLegend), isotypes or
389 *Maackia amurensis* Lectin II biotinylated (MAL-II, Vector Labs, San Diego, CA, USA)
390 coupled to Streptavidin (Biolegend), plus human BD Fc Block™ (BD Pharmingen™) and
391 Fixable Viability Stain (FVS, BD Horizon™, San Jose, CA, USA) were added to

392 leukocytes for 30 min at 4 $^{o}$C. Cells were washed, resuspended in FACS buffer,
393 acquired in a FACSVerse cytometer and analyzed using FlowJo software (FlowJo LLC).
394 Approximately 100.000 gated events were acquired in each analysis. *Phagocytosis*
395 *assays*. After RBCs lysis, 1 x $10^6$ leukocytes were incubated at 37 $^{o}$C (5% $CO_2$) or at 4
396 °C (control) with 100 µg/mL pHrodo™ Red *E. coli* BioParticles® (Thermo Fisher,
397 Waltham, MA, USA) for 60 min and the MFI of neutrophils ($FVS^-$/$CD66b^+$ cells) with
398 ingested bioparticle was analyzed by FACS. Total leukocytes were also incubated with
399 1 x $10^6$ CFU of live *E. coli* (ATCC 25922) for 90 min (37 $^{o}$C, 5% $CO_2$). Next, the cells
400 were washed twice (2 mM EDTA/PBS), fixed (FACS buffer/PFA 2%) and the
401 percentage of neutrophils with bacteria or the percentage of neutrophils with ≥3 bacteria
402 was analyzed by light microscopy using Differential Quick Stain Kit (Laborclin, Brazil).
403 *Bacterial killing*. Total leukocytes (1 x $10^6$) were incubated (37 $^{o}$C, 5% $CO_2$) with 1 x $10^6$
404 CFU of live *E. coli* for 180 min. The samples were centrifuged (270 g, 7 min, 4 $^{o}$C) and
405 10 µL of supernatant were diluted until $10^6$ and spread onto agar brain-heart infusion
406 (BHI, Kasvi, Brazil) to quantify the viable extracellular bacteria. The pellets were washed
407 twice with PBS/2 mM EDTA (270 g, 7 min, 4 $^{o}$C), the leukocytes were lysed with 2%
408 Triton-X, washed (PBS, 2000 g, 15 min, 4 $^{o}$C), resuspended in PBS and 10 µL of
409 samples were diluted until $10^6$ and spread onto agar BHI. Plates were incubated
410 overnight at 37 $^{o}$C and viable bacteria were expressed as mean ± SEM of CFU/mL.
411 *ROS assay*. After RBCs lysis, 1 x $10^6$ leukocytes were incubated at 37 $^{o}$C (5% $CO_2$) with
412 10 µM of cell-permeant 2',7'-dichlorodihydrofluorescein diacetate (CM-H2DCFDA,
413 ThermoFisher) for 5 min. Next, cells were stimulated or not with phorbol 12-myristate
414 13-acetate (PMA) for 10 min, fixed, washed twice with PBS/2 mM EDTA (270 g, 7 min,

415 4 °C) and analyzed by FACS. *NETs assay*. NETs quantification was performed as
416 previous described[68] on the supernatant of isolated neutrophils. Briefly, an anti-MPO
417 antibody bound to a 96-well flat-bottom plate captured the enzyme MPO (5 µg/ml;
418 Abcam), and the amount of DNA bound to the enzyme was quantified using the Quant-
419 iT™ PicoGreen® kit (Invitrogen, Carlsbad, CA, USA) according to the manufacturer's
420 instructions. Fluorescence intensity (Ex 488 nm/Em 525 nm) was quantified in a
421 FlexStation 3 Microplate Reader (Molecular Devices, San Jose, CA, USA). *Neutrophil*
422 *isolation*. Human circulating neutrophils were isolated by Percoll density gradients[69].
423 Briefly, four different gradients, 72%, 65%, 54%, and 45%, were used to isolate human
424 circulating neutrophils. After centrifugation at 600 g for 30 min at 4 °C, the cell layer at
425 the 72% gradient interface was collected as the neutrophil fraction. The erythrocytes
426 were removed by lysis, and cell pellets were resuspended in RPMI 1640. Isolated
427 neutrophils (1 x $10^6$/well) were treated with Oseltamivir, Zanamivir or medium 1 h before
428 the stimulus with PMA (50 nM) or LPS (10 µg/mL). After 4 hr of stimuli (37 °C, 5% $CO_2$),
429 the supernatant was collected to measure the levels of NETs.
430

431 **Neutrophil responses with plasma from COVID-19 patients**

432 Whole blood samples from sex-matched healthy donors (n = 7) were incubated for 2 h
433 (37 °C, 5% $CO_2$) with 7% of fresh plasma from healthy donors, severe or convalescent
434 COVID-19 patients or heat-inactivated plasma (56 °C, 30 min) from severe COVID-19
435 patients in the presence or absence of Oseltamivir (100 µM) or Zanamivir (30 µM).
436 Surface levels of α2-3-Sia and CD66b and ROS production were assessed on
437 neutrophils by FACS.

438

439 **Neuraminidase kinetics assay**

440 After RBCs lysis, 0.5 x $10^6$ leukocytes were resuspended in HBSS and added to 96-well
441 flat-bottom dark plate (SPL Life Sciences, South Korea) on ice. Then, 4-
442 Methylumbelliferyl-N-acetyl-α-D-Neuramic Acid (4-MU-NANA, Sigma-Aldrich) substrate
443 (0.025 mM) was added followed by medium, or LPS (1 µg/mL), LPS plus Oseltamivir
444 (100 µM), LPS plus Zanamivir (30 µM). CpNEU (10 mU), CpNEU plus Oseltamivir or
445 CpNEU plus Zanamivir were used as positive controls of the assay. The volume was
446 completed to 200 µL with HBSS, followed by reading on the Spectramax® Paradigm®
447 instrument starting 3 min after and every 5 min for 55 min at 37 ºC. Sialidase activity
448 was also assessed in heat-inactivated or fresh plasma from severe COVID-19 patients
449 in the presence or absence of Oseltamivir (100 µM) or Zanamivir (30 µM) using Tecan
450 Infinite 200 multi-reader. The fluorescent substrate 4-MU-NANA formation was detected
451 at ex 350 nm/em 450 nm.

452

453 **Mice**

454 The care and treatment of the animals were based on the Guide for the Care and Use
455 of Laboratory Animals[70] and all procedures followed the ARRIVE guidelines and the
456 international principles for laboratory animal studies[71]. C57BL/6 (Jackson Laboratory,
457 Bar Harbor, ME, USA) mice (8–10 weeks old) and Swiss mice (10–12 weeks old) were
458 housed in cages at 21 ± 2°C with free access to water and food at the Animal Facility of
459 the Department of Microbiology, Immunology, and Parasitology and Department of
460 Pharmacology from UFSC, respectively. A total of 228 mice were used in this study.

461 Protocols were approved by the Animal Use Ethics Committee of UFSC (CEUA
462 #8278290818).
463
464 ***E. coli-, Klebsiella pneumoniae-* and CLP-induced sepsis**
465 *E. coli* (ATCC 25922, Manassas, VA, USA) or *K. pneumoniae* (ATCC 700603) were
466 used to induce severe sepsis in mice. Naive mice were intraperitoneal (IP) challenged
467 with 100 µL of 1 x $10^7$ CFU of the *E. coli* suspension. A group of *E. coli*-septic mice was
468 randomly pretreated (2 hr before infection) and post treated by *per oral* (PO, 12/12 hr)
469 via with saline or Oseltamivir phosphate (10 mg/kg, Eurofarma, Brazil) for 4 days to
470 survival analysis. Another group was pretreated 2 hr before infection with a single dose
471 of Oseltamivir phosphate (10 mg/kg, PO) and the pathophysiological response was
472 analyzed at 4 and 6 hr after infection. *E. coli*-septic mice were also randomly
473 posttreated (6 hr after infection, 12/12 hr) with saline or Oseltamivir phosphate (PO, 10
474 mg/kg) for 4 days to survival analysis. For pneumonia-induced sepsis, mice were
475 anesthetized with isoflurane (3–5 vol%) and placed in supine position. A small incision
476 was made in the neck where the trachea could be localized and a *K. pneumoniae*
477 suspension (4 x $10^8$ CFU/50 µL of PBS) was injected into the trachea with a sterile 30-
478 gauge needle. Skin was sutured and animals were left for recovery in a warm cage.
479 After 6 hr of infection and then 12/12 hr mice were treated with Oseltamivir phosphate
480 (PO, 10 mg/kg) for survival analysis. In another set of experiments, pneumonia was
481 induced and mice were treated 6 hr after infection with a single dose of Oseltamivir
482 phosphate (10 mg/kg, PO) for material collection and analysis of pathophysiological
483 response 24 hr after infection.

484 Cecal ligation and puncture (CLP)-induced sepsis were performed as previously
485 described[28]. Mice were anesthetized with xylazine (2 mg/kg, IP, Syntec, Brazil) followed
486 by isoflurane (3–5 vol%, BioChimico, Brazil), a 1 cm midline incision was made in the
487 anterior abdomen, and the cecum was exposed and ligated below the ileocecal junction.
488 The cecum was punctured twice with an 18-gauge needle and gently squeezed to allow
489 its contents to be released through the punctures. Sham-operated (Sham) animals
490 underwent identical laparotomy but without cecal ligation and puncture. The cecum was
491 repositioned in the abdomen, and the peritoneal wall was closed. All animals received 1
492 mL of 0.9% saline subcutaneous (SC) and 100 μL of tramadol (5 mg/kg, SC, Vitalis,
493 Brazil) immediately after CLP. CLP-septic mice were randomly treated (starting 6 h after
494 infection, PO) with 100 μL of saline or Oseltamivir phosphate (10 mg/kg, 12/12 hr) for 4
495 days. In another set of experiments, CLP mice were randomly IP treated (6 hr after
496 infection, 12/12 hr) during 4 days with 100 μL metronidazole (15 mg/kg, Isofarma,
497 Brazil) plus ceftriaxone (40 mg/kg, Eurofarma, Brazil) and Oseltamivir phosphate (10
498 mg/kg) or saline by PO to survival analysis or treated for 36 hr to analyze the
499 pathophysiological response at 48 hr after CLP.

500 **Neutrophil migration**

501 The animals were euthanized in a $CO_2$ chamber, the bronchoalveolar lavage (BAL) and
502 peritoneal lavage (PL) were performed and the number of neutrophils was determined
503 at 4 and 6 hr after *E. coli*, 24 hr after *K. pneumoniae* infection or 48 hr after CLP
504 surgery, as described[28]. Next, mice were perfused with PBS/EDTA (1 mM) and the
505 lungs were harvested. Lungs were passed through 40-μm nylon cell strainers and

506 single-cell suspensions were centrifuged in 35% Percoll® solution (315 mOsm/kg,
507 Sigma-Aldrich) for 15 min at 700 g to enrich leukocytes populations. Pelleted cells were
508 then collected, and erythrocytes were lysed. Single-cell suspensions from individual
509 mice were determined using a cell counter (Coulter ACT, Beckman Coulter, Brea, CA,
510 USA) or with a haemocytometer. Differential counts were also determined on Cytospin
511 smears stained using Differential Quick Stain Kit (Laborclin, Brazil). Blood samples were
512 collected by heart puncture and tubes containing heparin for further analysis.
513 Neutrophils from LP or BAL were also stained with anti-Ly-6G/Ly-6C (GR-1, RB6-8C5;
514 BioLegend) and MAL-II to be further analyzed by FACS, as previously described.
515 Analysis was carried out in $SSC^{high}$/GR-$1^{high}$ cells.

516 **Bacterial counts**

517 The bacterial counts were determined as previously described[28]. Briefly, the BAL, PL or
518 blood were harvested and 10 µL of samples were plated on Muller-Hinton agar dishes
519 (Difco Laboratories, Waltham, MA, USA) and incubated for 24 hr at 37 °C. PL or BAL
520 samples were diluted until $10^6$.

521 **ELISA**

522 TNF (R&D Systems, Minneapolis, MN, USA) and IL-17 (XpressBio Life Sciences
523 Products, Frederick, MD, USA) levels in plasma, PL or BAL were determined by ELISA
524 kits according to the manufacturer's instructions.

525 **Tissue injury biochemical markers**

526 Aspartate aminotransferase (AST), alanine aminotransferase (ALT), alkaline
527 phosphatase (ALP) activities, and the levels of total bilirubin were determined in plasma
528 samples by commercial kits (Labtest Diagnóstica, Brazil). The procedures were carried
529 out according to the manufacturer's instructions.

530

531 **Lectin blotting of serum glycoproteins**

532 To evaluate if severe COVID-19 changes the α2-3 sialylation of serum glycoproteins,
533 serum samples from four healthy donors and five severe COVID-19 patients were
534 blotted with MAL-II as previously described[72]. Samples were diluted in SDS-PAGE
535 sample buffer and heated at 100 °C for 5 min. Twelve µg of total protein were resolved
536 in 10% SDS-PAGE and transferred onto nitrocellulose membranes (Millipore,
537 Burlington, MA, USA). Membranes were blocked (TBST + 5% BSA) overnight at 4 $^{o}$C
538 and incubated for 2 hr with 1 µg/mL of biotin-conjugated MAL-II, washed and incubated
539 for 40 min with alkaline-phosphatase (ALP)-conjugated streptavidin (Southern Biotec,
540 Birmingham, AL, USA) diluted 1:10.000. Both MAL-II and streptavidin-ALP were diluted
541 in TBST (5% BSA plus 150 mM of $CaCl_2$). Membranes were then revealed with
542 BCIP/NBT (5-bromo-4-chloro-3-indolyl-phosphate/nitro blue tetrazolium) color
543 development substrate (Promega, Brazil). The lane intensities were quantified using the
544 Image J software. In parallel, the resolved SDS-PAGE were stained with Coomassie
545 Brilliant blue R 250 (Merck KGaA, Germany) to compare the protein profile between the
546 different samples.

547

548 **Statistical analysis**

549 The data are reported as the mean or median ± SEM of the values obtained from two to
550 seven independent experiments. Each experiment using human samples was
551 performed using three to five samples from healthy donors or one to three samples from
552 severe or convalescent COVID-19 patients. We used five mice per experimental group
553 except for survival analyses in which twelve to twenty mice were used. The mean or
554 median values for the different groups were compared by analysis of variance (ANOVA)
555 followed by Dunnett and/or Tukey post-tests. Bacterial counts were analyzed by the
556 Mann–Whitney *U*-test or unpaired *t*-test using a parametric test with Welch's correction.
557 Survival curves were plotted using the Kaplan–Meier method and then compared using
558 the log-rank method and Gehan-Wilcoxon test. Data was analyzed using GraphPad
559 Prism version 8.00 for Mac (GraphPad Software, USA). A $P < 0.05$ was considered
560 significant.

561 **Abbreviations**

562 4-MU-NANA 4-methylumbelliferyl-N-acetyl-α -D-Neuramic Acid

563 ALP alkaline phosphatase

564 ALT alanine aminotransferase

565 ARRIVE Animal Research: Reporting of In Vivo Experiments

566 AST aspartate aminotransferase

567 ATCC American Type Culture Collection

568 BAL bronchoalveolar lavage

569 BHI brain–heart infusion

570 CD cluster of differentiation

571 CFU colony forming units

572 CLP cecal ligation and puncture

573 CM-H2DCFDA cell-permeant 2',7'-dichlorodihydrofluorescein diacetate

574 CpNEU *Clostridium perfringens* neuraminidase

575 DANA 2,3-dehydro-2-deoxy-N-acetylneuraminic acid

576 EDTA ethylenediamine tetra-acetic acid

577 FACS fluorescence-activated cell sorting

578 FcγR Fc gamma receptor

579 fMLP N-formyl-Met-Leu-Phe

580 FVS fixable viability stain

581 HBSS Hanks' balanced salt solution

582 IgG immunoglobulin G

583 IP intraperitoneal pathway

584 LPS lipopolysaccharide

585 MAL-II *Maackia amurensis* lectin II

586 MFI median fluorescence intensity

587 NETs neutrophil extracellular traps

588 NEU neuraminidases

589 Neu5Ac2en 2-deoxy-2, 3-didehydro-D-N-acetylneuraminic acid

590 PBS phosphate buffered saline

591 PFA paraformaldehyde

592 PL peritoneal lavage

593 PMA 12-myristate 13-acetate

594 PMN polymorphonuclear

595 PO oral pathway

596 RBCs red blood cells

597 ROS reactive oxygen species

598 SARS-CoV-2 severe acute respiratory syndrome coronavirus 2

599 SC subcutaneous pathway

600 Sia sialic acids

601 Siglecs sialic acid-binding immunoglobulin-like lectins

602 TLR toll-like receptor

603 COVID-19 coronavirus disease 2019

604 WT wild-type

605 **Acknowledgments**

606 We thank UFSC microscopy (LCME) and biology (LAMEB) facilities for technical
607 support.

608

609 **Authors' contributions**

610 All named authors meet the criteria for authorship of this manuscript, take responsibility
611 for the work's integrity as a whole, and have given final approval for publication.

612

613 ROF, FCA, DM, RS, DSM, AB, MSM and FS designed experiments and analyzed data;
614 ROF, FAC, CFS, DM, CWW, CLB, AAS, JA, LFF, CCN, NMP, PCS, FRF, FAS, LA, NH,
615 AB and FS performed experiments; SB, AM, MSM, FQC and RM contributed with
616 critical reagents/tools/clinical samples; ROF, FS, AB wrote the manuscript.

617

618 **Competing Interests statement**

619 The authors declare that no conflict of interest exists.

620

621 **Funding**

622 This work was funded by FAPESP-SCRIPPS (FS; 15/50387-4), Howard Hughes
623 Medical Institute – Early Career Scientist (AB; 55007412), National Institutes of Health
624 Global Research Initiative Program (AB; TW008276), CAPES Computational Biology
625 (DSM; 23038.010048/2013–27), CNPQ/COVID-19 (AB; 401209/2020-2), CNPQ/PQ
626 Scholars (AB and DSM), FAPESC Scholarship (DM).

627 **REFERENCES**


628 1. Mócsai, A. Diverse novel functions of neutrophils in immunity, inflammation, and beyond. *J.*
629 *Exp. Med.* **210**, 1283–1299 (2013).
630 2. Veras, F. P. *et al.* SARS-CoV-2-triggered neutrophil extracellular traps mediate COVID-19
631 pathology. *J. Exp. Med.* **217**, (2020).
632 3. Alves-Filho, J. C., Spiller, F. & Cunha, F. Q. Neutrophil paralysis in sepsis. *Shock* **34 Suppl**
633 **1**, 15–21 (2010).
634 4. Segal, A. W. How neutrophils kill microbes. *Annu. Rev. Immunol.* **23**, 197–223 (2005).
635 5. Steevels, T. A. M. & Meyaard, L. Immune inhibitory receptors: essential regulators of
636 phagocyte function. *Eur. J. Immunol.* **41**, 575–587 (2011).
637 6. Macauley, M. S., Crocker, P. R. & Paulson, J. C. Siglec-mediated regulation of immune cell
638 function in disease. *Nat. Rev. Immunol.* **14**, 653–666 (2014).
639 7. Chang, Y.-C., Uchiyama, S., Varki, A. & Nizet, V. Leukocyte inflammatory responses
640 provoked by pneumococcal sialidase. *MBio* **3**, (2012).
641 8. Varki, A. Sialic acids in human health and disease. *Trends. Mol. Med.* **14,** 351–360 (2008).
642 9. Lipničanová, S., Chmelová, D., Ondrejovič, M., Frecer, V. & Miertuš, S. Diversity of
643 sialidases found in the human body - A review. *Int. J. Biol. Macromol.* **148**, 857–868 (2020).
644 10. Varki, A. & Gagneux, P. Multifarious roles of sialic acids in immunity. *Ann. N. Y. Acad. Sci.*
645 **1253**, 16–36 (2012).
646 11. Suzuki, H., Kurita, T. & Kakinuma, K. Effects of neuraminidase on O2 consumption and
647 release of O2 and H2O2 from phagocytosing human polymorphonuclear leukocytes. *Blood*
648 **60,** 446–453 (1982).
649 12. Arora, D. J. S. & Henrichon, M. Superoxide Anion Production in Influenza Protein-Activated
650 NADPH Oxidase of Human Polymorphonuclear Leukocytes. *J. Infect. Dis.* **169**, 1129–1133
651 (1994).

652 13. Henricks, P. A., van Erne-van der Tol, M. E. & Verhoef, J. Partial removal of sialic acid
653 enhances phagocytosis and the generation of superoxide and chemiluminescence by
654 polymorphonuclear leukocytes. *J. Immunol.* **129**, 745–750 (1982).
655 14. Amith, S. R. *et al.* Dependence of pathogen molecule-induced Toll-like receptor activation
656 and cell function on Neu1 sialidase. *Glycoconj. J.* **26**, 1197–1212 (2009).
657 15. Yang, W. H. *et al.* Accelerated Aging and Clearance of Host Anti-inflammatory Enzymes by
658 Discrete Pathogens Fuels Sepsis. *Cell. Host. Microbe.* **24**, 500–513.e5 (2018).
659 16. Chen, G.-Y. *et al.* Broad and direct interaction between TLR and Siglec families of pattern
660 recognition receptors and its regulation by Neu1. *Elife* **3**, e04066 (2014).
661 17. Mills, E. L., Debets-Ossenkopp, Y., Verbrugh, H. A. & Verhoef, J. Initiation of the respiratory
662 burst of human neutrophils by influenza virus. *Infect. Immun.* **32**, 1200–1205 (1981).
663 18. Mondal, N. *et al.* ST3Gal-4 is the primary sialyltransferase regulating the synthesis of E-, P-
664 , and L-selectin ligands on human myeloid leukocytes. *Blood* **125,** 687–696 (2015).
665 19. Knibbs, R. N., Goldstein, I. J., Ratcliffe, R. M. & Shibuya, N. Characterization of the
666 carbohydrate binding specificity of the leukoagglutinating lectin from Maackia amurensis.
667 Comparison with other sialic acid-specific lectins. *J. Biol. Chem.* **266**, 83–88 (1991).
668 20. Movsisyan, L. D. & Macauley, M. S. Structural advances of Siglecs: insight into synthetic
669 glycan ligands for immunomodulation. *Org. Biomol. Chem.* **18**, 5784–5797 (2020).
670 21. Cross, A. S. & Wright, D. G. Mobilization of sialidase from intracellular stores to the surface
671 of human neutrophils and its role in stimulated adhesion responses of these cells. *J. Clin.*
672 *Invest.* **88**, 2067–2076 (1991).
673 22. Schmidt, T. *et al.* CD66b overexpression and homotypic aggregation of human peripheral
674 blood neutrophils after activation by a gram-positive stimulus. *J. Leukoc. Biol.* **91**, 791–802
675 (2012).
676 23. Kishimoto, T. K., Jutila, M. A., Berg, E. L. & Butcher, E. C. Neutrophil Mac-1 and MEL-14
677 adhesion proteins inversely regulated by chemotactic factors. *Science* **245**, 1238–1241

678 (1989).
679 24. Jutila, M. A., Rott, L., Berg, E. L. & Butcher, E. C. Function and regulation of the neutrophil
680 MEL-14 antigen in vivo: comparison with LFA-1 and MAC-1. *J. Immunol.* **143**, 3318–3324
681 (1989).
682 25. Amith, S. R. *et al.* Neu1 desialylation of sialyl alpha-2,3-linked beta-galactosyl residues of
683 TOLL-like receptor 4 is essential for receptor activation and cellular signaling. *Cell. Signal.*
684 **22**, 314–324 (2010).
685 26. Mittal, M., Siddiqui, M. R., Tran, K., Reddy, S. P. & Malik, A. B. Reactive oxygen species in
686 inflammation and tissue injury. *Antioxid. Redox Signal.* **20**, 1126–1167 (2014).
687 27. Sônego, F. *et al.* Paradoxical Roles of the Neutrophil in Sepsis: Protective and Deleterious.
688 *Front. Immunol.* **7**, 155 (2016).
689 28. Spiller, F. *et al.* Hydrogen Sulfide Improves Neutrophil Migration and Survival in Sepsis via
690 K ATPChannel Activation. *Am. J. Respir. Crit. Care Med.* **182**, 360–368 (2010).
691 29. Spiller, F. *et al.* 1-Acid Glycoprotein Decreases Neutrophil Migration and Increases
692 Susceptibility to Sepsis in Diabetic Mice. *Diabetes* **61**, 1584–1591 (2012).
693 30. Vimr, E. R. & Troy, F. A. Identification of an inducible catabolic system for sialic acids (nan)
694 in Escherichia coli. *J. Bacteriol.* **164**, 845–853 (1985).
695 31. Butler, C. C. *et al.* Oseltamivir plus usual care versus usual care for influenza-like illness in
696 primary care: an open-label, pragmatic, randomised controlled trial. *Lancet* **395**, 42–52
697 (2020).
698 32. Rittirsch, D., Huber-Lang, M. S., Flierl, M. A. & Ward, P. A. Immunodesign of experimental
699 sepsis by cecal ligation and puncture. *Nat. Protoc.* **4**, 31–36 (2009).
700 33. Rhodes, A. *et al.* Surviving Sepsis Campaign: International Guidelines for Management of
701 Sepsis and Septic Shock: 2016. *Crit. Care Med.* **45**, 486–552 (2017).
702 34. Chou, E. H. *et al.* Incidence, trends, and outcomes of infection sites among hospitalizations
703 of sepsis: A nationwide study. *PLoS One* **15**, e0227752 (2020).

704 35. Middleton, E. A. *et al.* Neutrophil extracellular traps contribute to immunothrombosis in
705 COVID-19 acute respiratory distress syndrome. *Blood* **136**, 1169–1179 (2020).
706 36. Schurink, B. *et al.* Viral presence and immunopathology in patients with lethal COVID-19: a
707 prospective autopsy cohort study. *Lancet Microbe*. **7**, e290-e299 (2020).
708 37. Huang, C. *et al.* Clinical features of patients infected with 2019 novel coronavirus in Wuhan,
709 China. *Lancet* **395**, 497–506 (2020).
710 38. Guan, W.-J. *et al.* Clinical Characteristics of Coronavirus Disease 2019 in China. *N. Engl. J.*
711 *Med.* **382**, 1708–1720 (2020).
712 39. Silvin, A. *et al.* Elevated Calprotectin and Abnormal Myeloid Cell Subsets Discriminate
713 Severe from Mild COVID-19. *Cell* **182**, 1401–1418.e18 (2020).
714 40. Wilk, A. J. *et al.* A single-cell atlas of the peripheral immune response in patients with
715 severe COVID-19. *Nat. Med.* **26**, 1070–1076 (2020).
716 41. Kuri-Cervantes, L. *et al.* Comprehensive mapping of immune perturbations associated with
717 severe COVID-19. *Sci Immunol* **5**, (2020).
718 42. Schulte-Schrepping, J. *et al.* Severe COVID-19 Is Marked by a Dysregulated Myeloid Cell
719 Compartment. *Cell* **182**, 1419–1440.e23 (2020).
720 43. Leliefeld, P. H. C., Wessels, C. M., Leenen, L. P. H., Koenderman, L. & Pillay, J. The role of
721 neutrophils in immune dysfunction during severe inflammation. *Crit. Care* **20**, 73 (2016).
722 44. Smutova, V. *et al.* Structural basis for substrate specificity of mammalian neuraminidases.
723 *PLoS One* **9**, e106320 (2014).
724 45. Glanz, V. Y., Myasoedova, V. A., Grechko, A. V. & Orekhov, A. N. Sialidase activity in
725 human pathologies. *Eur. J. Pharmacol.* **842**, 345–350 (2019).
726 46. Cross, A. S. *et al.* Recruitment of murine neutrophils in vivo through endogenous sialidase
727 activity. *J. Biol. Chem.* **278**, 4112–4120 (2003).
728 47. Pshezhetsky, A. V. & Hinek, A. Where catabolism meets signalling: neuraminidase 1 as a
729 modulator of cell receptors. *Glycoconj. J.* **28**, 441–452 (2011).

730 48. Abdulkhalek, S. *et al.* Neu1 sialidase and matrix metalloproteinase-9 cross-talk is essential
731 for Toll-like receptor activation and cellular signaling. *J. Biol. Chem.* **286**, 36532–36549
732 (2011).
733 49. Feng, C. *et al.* Sialyl residues modulate LPS-mediated signaling through the Toll-like
734 receptor 4 complex. *PLoS One* **7**, e32359 (2012).
735 50. Blander, J. M. & Medzhitov, R. Regulation of phagosome maturation by signals from toll-
736 like receptors. *Science* **304**, 1014–1018 (2004).
737 51. Doyle, S. E. *et al.* Toll-like receptors induce a phagocytic gene program through p38. *J.*
738 *Exp. Med.* **199**, 81–90 (2004).
739 52. El-Benna, J., Dang, P. M.-C. & Gougerot-Pocidalo, M.-A. Priming of the neutrophil NADPH
740 oxidase activation: role of p47phox phosphorylation and NOX2 mobilization to the plasma
741 membrane. *Semin. Immunopathol.* **30**, 279–289 (2008).
742 53. Brinkmann, V. Neutrophil Extracellular Traps Kill Bacteria. *Science* **303**, 1532–1535 (2004).
743 54. Böhmer, R. H., Trinkle, L. S. & Staneck, J. L. Dose effects of LPS on neutrophils- in a
744 whole blood flow cytometric assay of phagocytosis and oxidative burst. *Cytometry* **13**, 525–
745 531 (1992).
746 55. Rifat, S. *et al.* Expression of sialyltransferase activity on intact human neutrophils. *J.*
747 *Leukoc. Biol.* **84**, 1075–1081 (2008).
748 56. Cross, A. S. *et al.* Recruitment of Murine Neutrophils in Vivo through Endogenous Sialidase
749 Activity. *J. Biol. Chem.* **278**, 4112–4120 (2003).
750 57. Feng, C. *et al.* Endogenous PMN sialidase activity exposes activation epitope on
751 CD11b/CD18 which enhances its binding interaction with ICAM-1. *J. Leukoc. Biol.* **90**, 313–
752 321 (2011).
753 58. Sakarya, S. *et al.* Mobilization of neutrophil sialidase activity desialylates the pulmonary
754 vascular endothelial surface and increases resting neutrophil adhesion to and migration
755 across the endothelium. *Glycobiology* **14**, 481–494 (2004).

756 59. Petri, B., Phillipson, M. & Kubes, P. The Physiology of Leukocyte Recruitment: An In Vivo
757 Perspective. *J. Immunol.* **180**, 6439–6446 (2008).
758 60. Worthen, G., Schwab, B., Elson, E. & Downey, G. Mechanics of stimulated neutrophils: cell
759 stiffening induces retention in capillaries. *Science* **245**, 183–186 (1989).
760 61. Sheu, C.-C. *et al.* Clinical characteristics and outcomes of sepsis-related vs non-sepsis-
761 related ARDS. *Chest* **138**, 559–567 (2010).
762 62. Wang, T. *et al.* Comorbidities and multi-organ injuries in the treatment of COVID-19. *Lancet*
763 **395**, e52 (2020).
764 63. Wu, Z. & McGoogan, J. M. Characteristics of and Important Lessons From the Coronavirus
765 Disease 2019 (COVID-19) Outbreak in China: Summary of a Report of 72 314 Cases From
766 the Chinese Center for Disease Control and Prevention. *JAMA* **323**, 1239–1242 (2020).
767 64. Hottz, E. D. *et al.* Platelet activation and platelet-monocyte aggregate formation trigger
768 tissue factor expression in patients with severe COVID-19. *Blood* **136**, 1330–1341 (2020).
769 65. Wang, J., Jiang, M., Chen, X. & Montaner, L. J. Cytokine storm and leukocyte changes in
770 mild versus severe SARS- CoV- 2 infection: Review of 3939 COVID- 19 patients in China
771 and emerging pathogenesis and therapy concepts. *J. Leukoc. Biol.* **108**, 17–41 (2020).
772 66. Vogl, T. *et al.* Autoinhibitory regulation of S100A8/S100A9 alarmin activity locally restricts
773 sterile inflammation. *J. Clin. Invest.* **128**, 1852–1866 (2018).
774 67. Liu, J. *et al.* Clinical outcomes of COVID-19 in Wuhan, China: a large cohort study. *Ann.*
775 *Intensive Care* **10**, 99 (2020).
776 68. Czaikoski, P. G. *et al.* Neutrophil Extracellular Traps Induce Organ Damage during
777 Experimental and Clinical Sepsis. *PLoS One* **11**, e0148142 (2016).
778 69. Mestriner, F. L. A. C. *et al.* Acute-phase protein alpha-1-acid glycoprotein mediates
779 neutrophil migration failure in sepsis by a nitric oxide-dependent mechanism. *Proc. Natl.*
780 *Acad. Sci. U. S. A.* **104**, 19595–19600 (2007).
781 70. National Research Council, Division on Earth and Life Studies, Institute for Laboratory

782 Animal Research & Committee for the Update of the Guide for the Care and Use of
783 Laboratory Animals. *Guide for the Care and Use of Laboratory Animals: Eighth Edition*.
784 (National Academies Press, 2011).
785 71. Kilkenny, C., Browne, W. J., Cuthill, I. C., Emerson, M. & Altman, D. G. Improving
786 bioscience research reporting: the ARRIVE guidelines for reporting animal research. *PLoS*
787 *Biol.* **8**, e1000412 (2010).
788 72. Xu, J. *et al.* A fixation method for the optimisation of western blotting. *Sci. Rep.* **9**, 6649
789 (2019).

790

791 **Figures and Figure Legends**
792

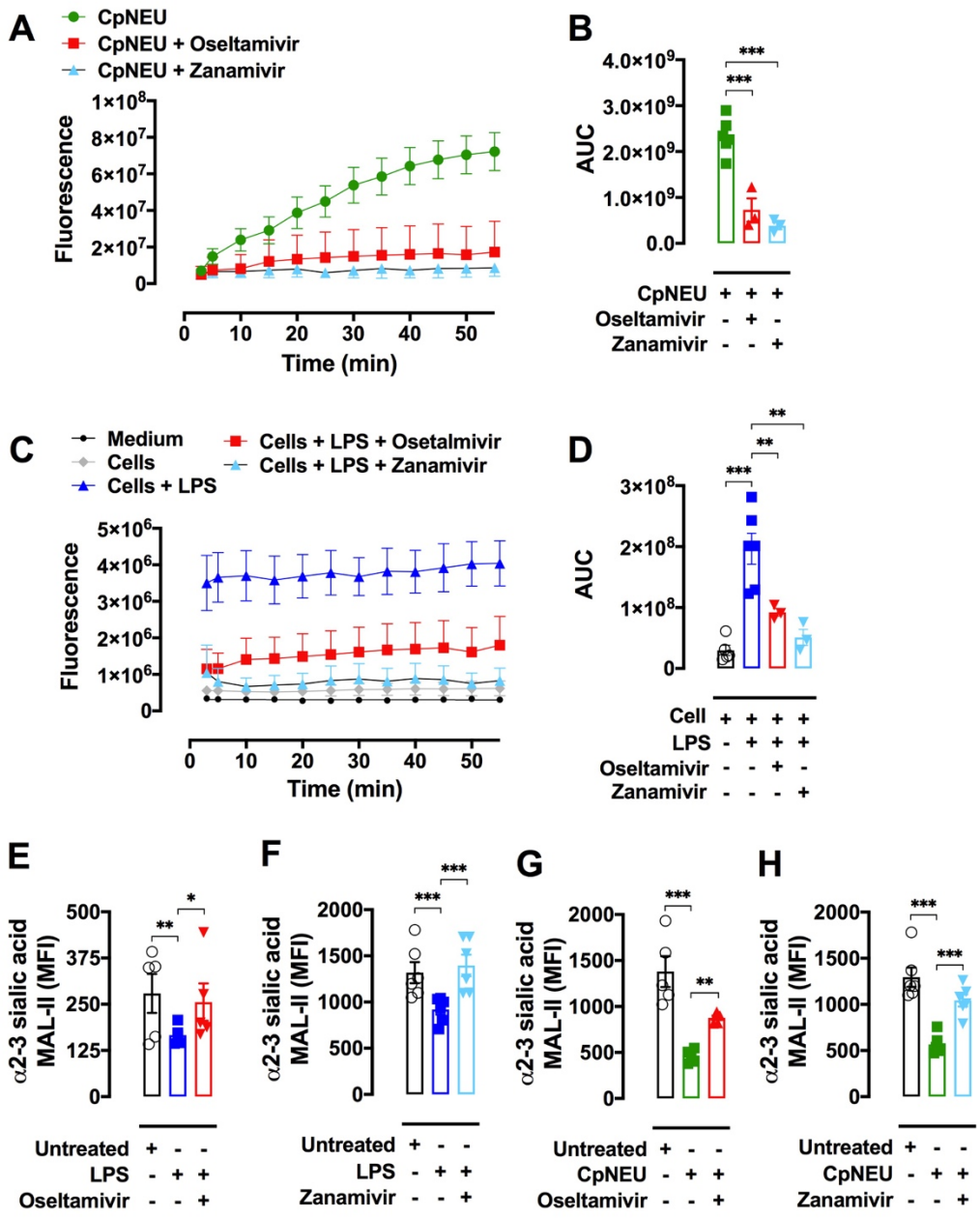


793
794

795 **Figure 1. LPS stimulates NEU activity in human leukocytes.** Neuraminidase isolated
796 from *Clostridium perfringens* (CpNEU) was used to validate the NEU activity assay.
797 CpNEU (0.012 UI) was added in a 96-well flat-bottom dark plate on ice in the presence
798 or not of its inhibitors Oseltamivir phosphate (100 μM) or Zanamivir (30 μM). Next, the
799 substrate 4-MU-NANA (0.025 mM) was added and the fluorescent substrate was read 3
800 min after at 37 ºC (**A**). The area under the curve (AUC) values are shown in **B**. Total

801 leukocytes resuspended in HBSS were added in a plate on ice and 4-MU-NANA
802 substrate (0.025 mM) was added followed by the addition of medium, LPS (1 μg/mL),
803 LPS plus Oseltamivir (100 μM) or LPS plus Zanamivir (30 μM). The fluorescent
804 substrate was read 3 min after at 37 ºC (**C**). Raw data were subtracted from the control
805 group containing only HBSS (medium) and expressed as AUC values (**D**). Whole blood
806 containing 1 x $10^6$ leukocytes from healthy donors were stimulated or not with LPS (1
807 μg/mL, 90 min, 37 $^oC$, 5% $CO_2$), LPS plus Oseltamivir (100 μM), or LPS plus Zanamivir
808 (30 μM). Total leukocytes (1 x $10^6$) were incubated with CpNEU (10 mU, 60 min, 37 $^oC$,
809 5% $CO_2$), CpNEU plus Oseltamivir (100 μM), or CpNEU plus Zanamivir (30 μM).
810 Leukocytes were stained with MAL-II to detect α2-3 sialic acids (**E-F**). The MFI was
811 analyzed on $CD66b^+$ cells using the gate strategies shown in Supplementary Fig. 1. *$P$
812 < 0.05; **$P$ < 0.01; ***$P$ < 0.001. This figure is representative of three independent
813 experiments (n= 3-6) and data are shown as mean ± SEM. LPS = lipopolysaccharide;
814 MAL-II = *Maackia amurensis* lectin II; CpNEU = neuraminidase.
815

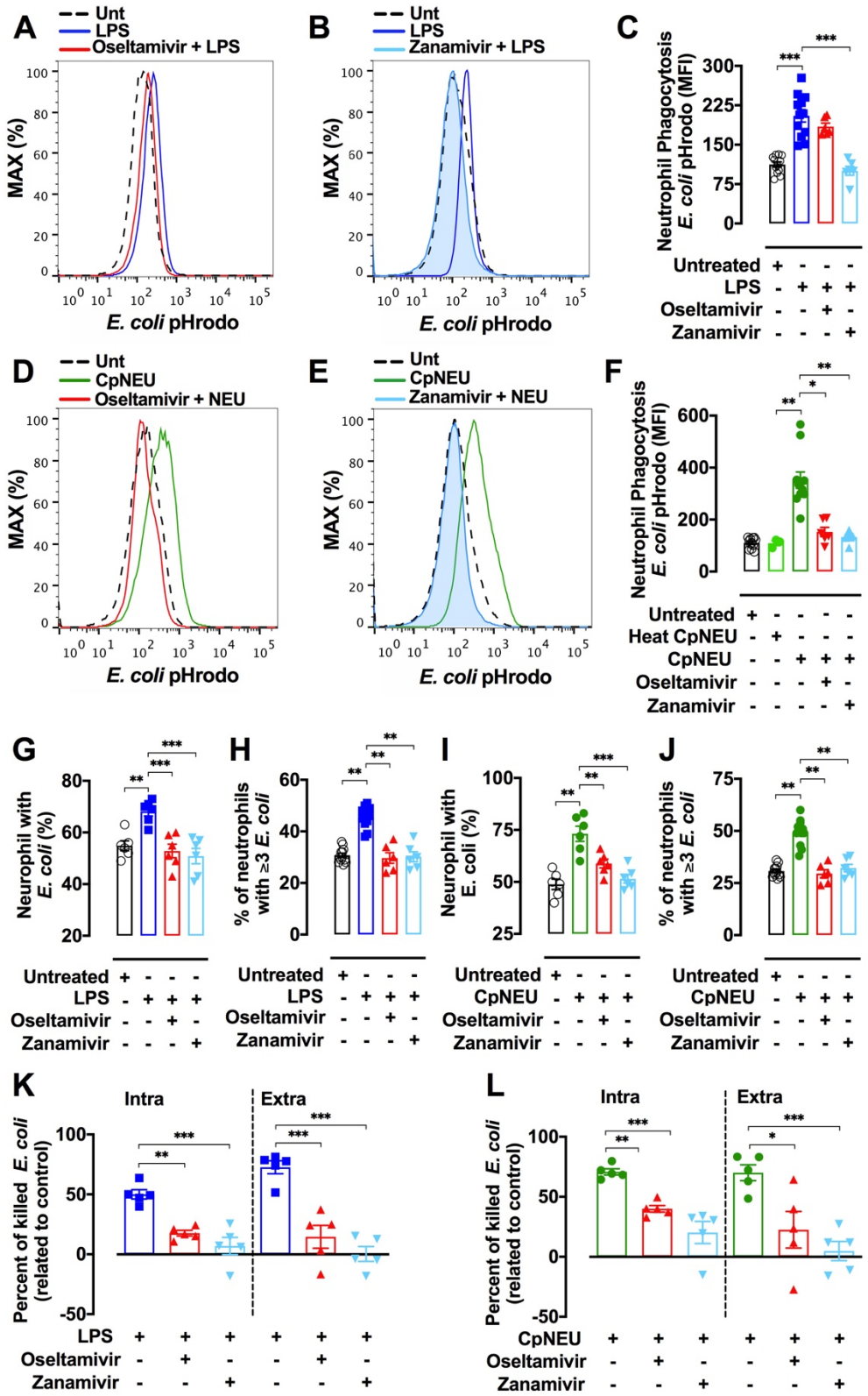


816

817 **Figure 2. LPS increases phagocytosis and killing of *E. coli* in a NEU-dependent**
818 **manner.** Whole blood from healthy donors containing 1 x $10^6$ leukocytes were exposed

819 (37 $^{o}$C, 5% $CO_2$) or not to LPS (1 µg/mL, 90 min), LPS plus Oseltamivir (100 µM), or
820 LPS plus Zanamivir (30 µM) (**A-C; G-H; K**). Total leukocytes (1 x $10^6$) were exposed or
821 not to CpNEU (10 mU, 60 min, 37 $^{o}$C, 5% $CO_2$), CpNEU plus Oseltamivir (100 µM), or
822 CpNEU plus Zanamivir (30 µM) (**D-F; I-J; L**) and the phagocytosis and killing assays
823 were performed. Leukocytes were incubated with *E. coli* pHrodo BioParticles® (100
824 µg/mL) for 60 min at 37 °C to assess phagocytosis in viable CD66b$^+$ cells (**A-F**) (as
825 gated in Supplementary Fig. 1). Live *E. coli* was used to evaluate phagocytosis by light
826 microscopy or to assess the killing by leukocytes. Cells were stimulated as described
827 above and 1 x$10^6$ leukocytes were incubated at 37 °C with *E. coli* (1 x$10^6$ CFU) for 90
828 min for phagocytosis or for 180 min for killing assays. The percentage of cells with
829 ingested bacteria (**G; I**) and the number of bacterial particles per cell (**H; J**, ≥3 particles
830 per cell) were evaluated. The killing of *E. coli* was evaluated by spreading 10 µL of
831 supernatant (extracellular killing) or 10 µL of the intracellular content in agar medium
832 and the CFU were counted. Killing *E. coli* was expressed as the rate of fold change
833 compared to the unprimed (untreated) cells (**L**). Symbols represent individual donors
834 and data are shown as mean ± SEM from pooled data of two to three independent
835 experiments (n = 3-12). *$P < 0.05$; **$P < 0.01$; ***$P < 0.001$. Unt = untreated; LPS =
836 lipopolysaccharide; CpNEU = neuraminidase.
837
838

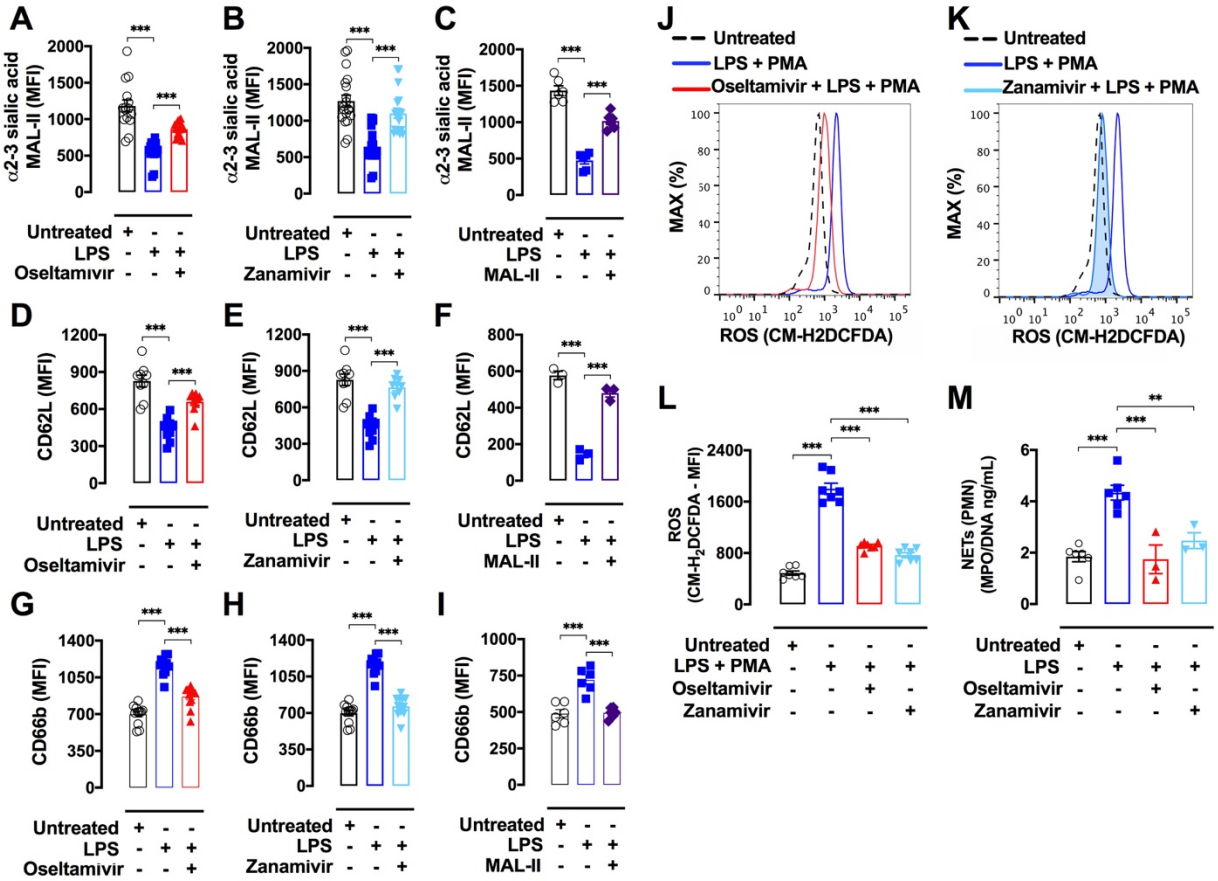


**Figure 3. LPS-induced human neutrophil response involves NEU activity.** Whole blood from healthy donors containing 1 x $10^6$ leukocytes were stimulated or not with LPS (1 µg/mL, 90 min, 37 °C, 5% $CO_2$), LPS plus Oseltamivir (100 µM), LPS plus Zanamivir (30 µM), or LPS plus MAL-II (1 µg/mL, MAL-II promotes steric hindrance at the NEU cleavage site and prevent sialic acid cleavage). Leukocytes were marked with MAL-II to detect α2-3 sialic acids (**A-C**) or stained with the cell activation markers CD62L (**D-F**) and CD66b (**G-I**). After RBCs lysis leukocytes were incubated with 5 µM CM-H2DCFDA fluorescent probe for 15 min. PMA (10 µM) was used to stimulate ROS production for 10 min (**J-L**). Supplementary Fig. 5 showed ROS production in additional control groups. The MFI was analyzed on $CD66b^+$ cells using the gate strategies shown in Supplementary Fig. 1. Isolated neutrophils were treated with Osetamivir (100 µM) or Zanamivir (30 µM) 1 h before the stimulus with LPS (10 µg/mL) for 4 h. The concentration of NETs was evaluated by MPO-DNA PicoGreen assay on supernatants

855 of cells (**M**). Symbols represent individual donors and data are shown as mean ± SEM
856 from pooled data of two to three independent experiments (n = 7) except for F and M
857 that was made once with n=3. ***$P < 0.001$; **$P < 0.01$. Unt = untreated; CM-H2DCFDA
858 = 5-(and-6)-chloromethyl-2',7'-dichlorodihydrofluorescein diacetate, acetyl ester; LPS =
859 lipopolysaccharide; PMA = phorbol 12-myristate 13-acetate; ROS = reactive oxygen
860 species; NETs = neutrophil extracellular traps; RBCs = red blood cells; MAL-II =
861 *Maackia amurensis* lectin II; PMN = polymorphonuclear leukocytes.

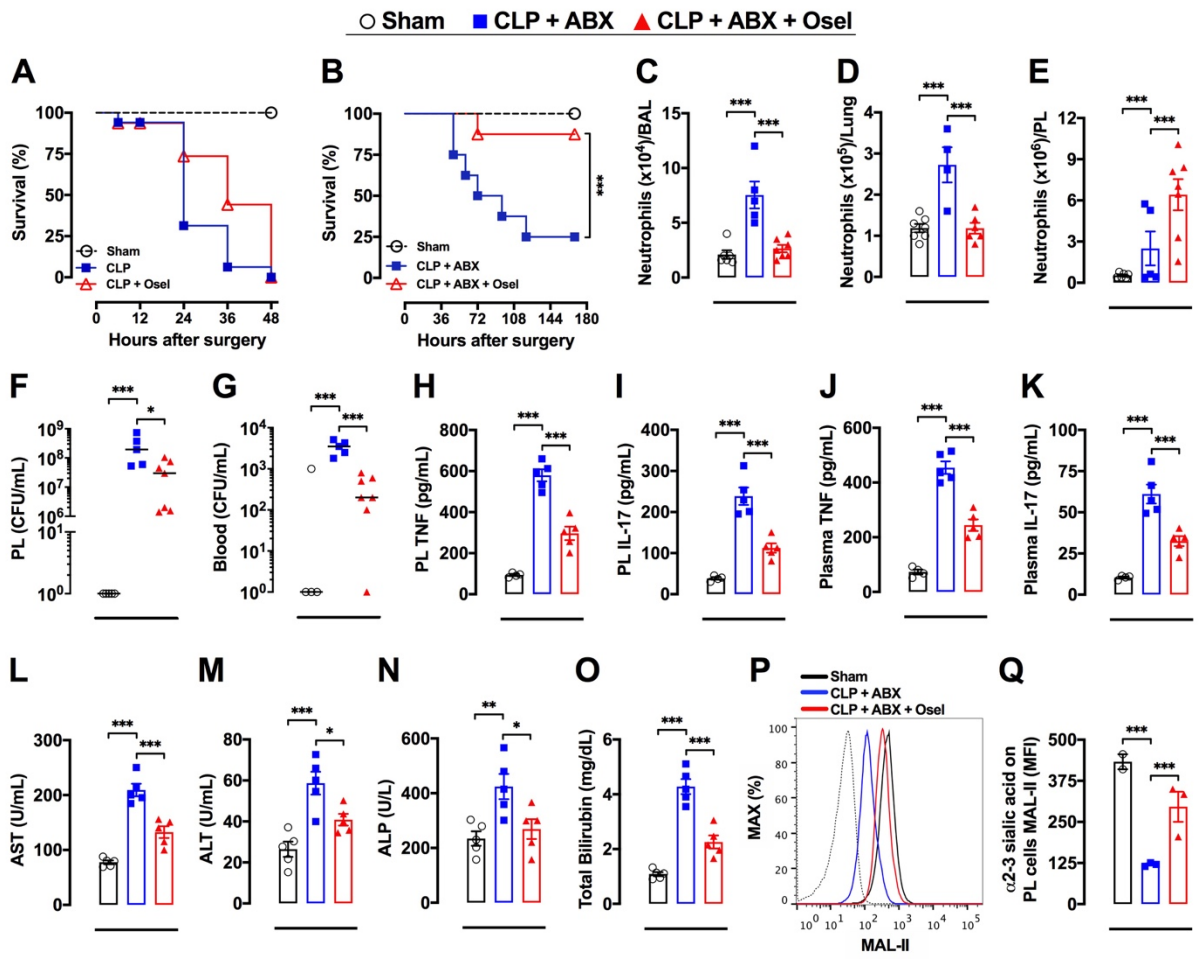


**Figure 4. Oseltamivir enhanced host survival in CLP-induced sepsis.** Severe sepsis was induced by the cecal ligation and puncture (CLP) model. Mice were randomly treated (starting 6 hr after infection, 12/12 h, PO, for 36 hr, n=16) with saline or Oseltamivir phosphate (10 mg/kg) and their survival rates were monitored over 48 hr (**A**). In another set of experiments, CLP mice were randomly IP treated (started 6 hr after infection, 12/12 hr) during 4 days with 100 µL metronidazole (15 mg/kg)/ceftriaxone (40 mg/kg) (ABX) plus saline or Oseltamivir phosphate (10 mg/kg) by PO and their survival rates (n=12) were monitored over 168 hr (**B**). Also, mice were subjected to CLP and treated with ABX + saline or ABX + Olsetamivir as described in B and euthanized 48 hr after surgery to evaluate the number of neutrophils in BAL (**C**), lung tissue (**D**), and peritoneal lavage (PL) (**E**); TNF (**H**), IL-17 (**I**), and CFU (**F**) were also determined in PL. Blood CFU (**G**) and plasmatic levels of TNF (**J**), IL-17 (**K**), AST (**L**), ALT (**M**), ALP (**N**) and total bilirubin (**O**) were also evaluated 48 hr after surgery.

877 The amount of surface α2-3 sialic acids were assessed by MAL-II staining in
878 $SSC^{high}$/Gr-$1^{high}$ cells in PL and analyzed by FACS, as shown by the representative
879 histograms (**P**) and MFI (**Q**); dotted line = unstained cells. The results are expressed as
880 percent of survival (n=16), mean or median (only for FACS data) ± SEM. *$P < 0.05$; ***$P$
881 $< 0.001$. These experiments were repeated 3 times for survival analysis and twice for
882 other parameters (n=3-7). ABX = antibiotics (metronidazole/ceftriaxone); Sham = sham-
883 operated. Osel = Oseltamivir; AST = alanine aminotransferase; ALT = aspartate
884 aminotransferase; ALP = alkaline phosphatase; CFU = colony-forming units.

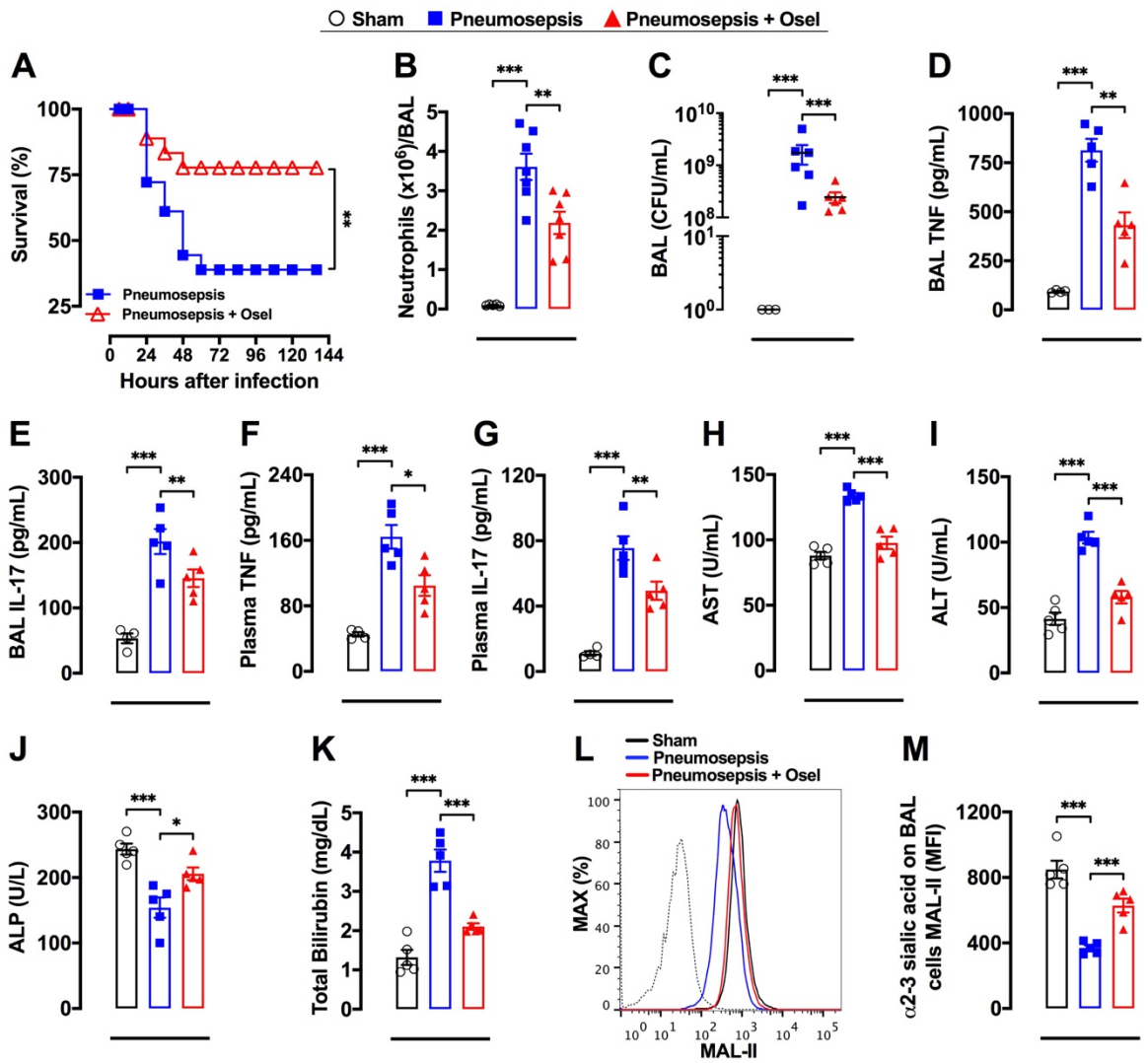


**Figure 5. Oseltamivir enhanced mice survival in *K. pneumoniae*-induced sepsis.** Sepsis was induced by intratracheal administration of *K. pneumoniae* and mice were randomly treated (starting 6 hr after infection, 12/12 hr, PO, n=20) with saline or Oseltamivir phosphate (10 mg/kg) and survival rates were monitored for 144 hr (**A**). In similar set of experiments, septic mice (n=6-7) were treated 6 hr after infection with a single dose of Oseltamivir phosphate (10 mg/kg, PO) and mice were euthanized 24 hr after infection to determine the number of neutrophils (**B**) and CFUs (**C**), and levels of TNF (**D**) and IL-17 (**E**) in BAL. Plasma levels of TNF (**F**), IL-17 (**G**), AST (**H**), ALT (**I**), ALP (**J**) and total bilirubin (**K**) were also evaluated 24 hr after infection. The amount of surface α2-3 sialic acids were assessed by MAL-II staining in $SSC^{high}$/Gr-$1^{high}$ cells in BAL and analyzed by FACS, as shown by the representative histograms (**L**) and MFI

897 (**M**); dotted line = unstained cells. The results are expressed as percent of survival,
898 mean or median (only for FACS data) ± SEM. *$P < 0.05$; *$P < 0.01$; ***$P < 0.001$. Sham
899 = sham-operated mice; Osel = Oseltamivir; AST = alanine aminotransferase; ALT =
900 aspartate aminotransferase; ALP = alkaline phosphatase.

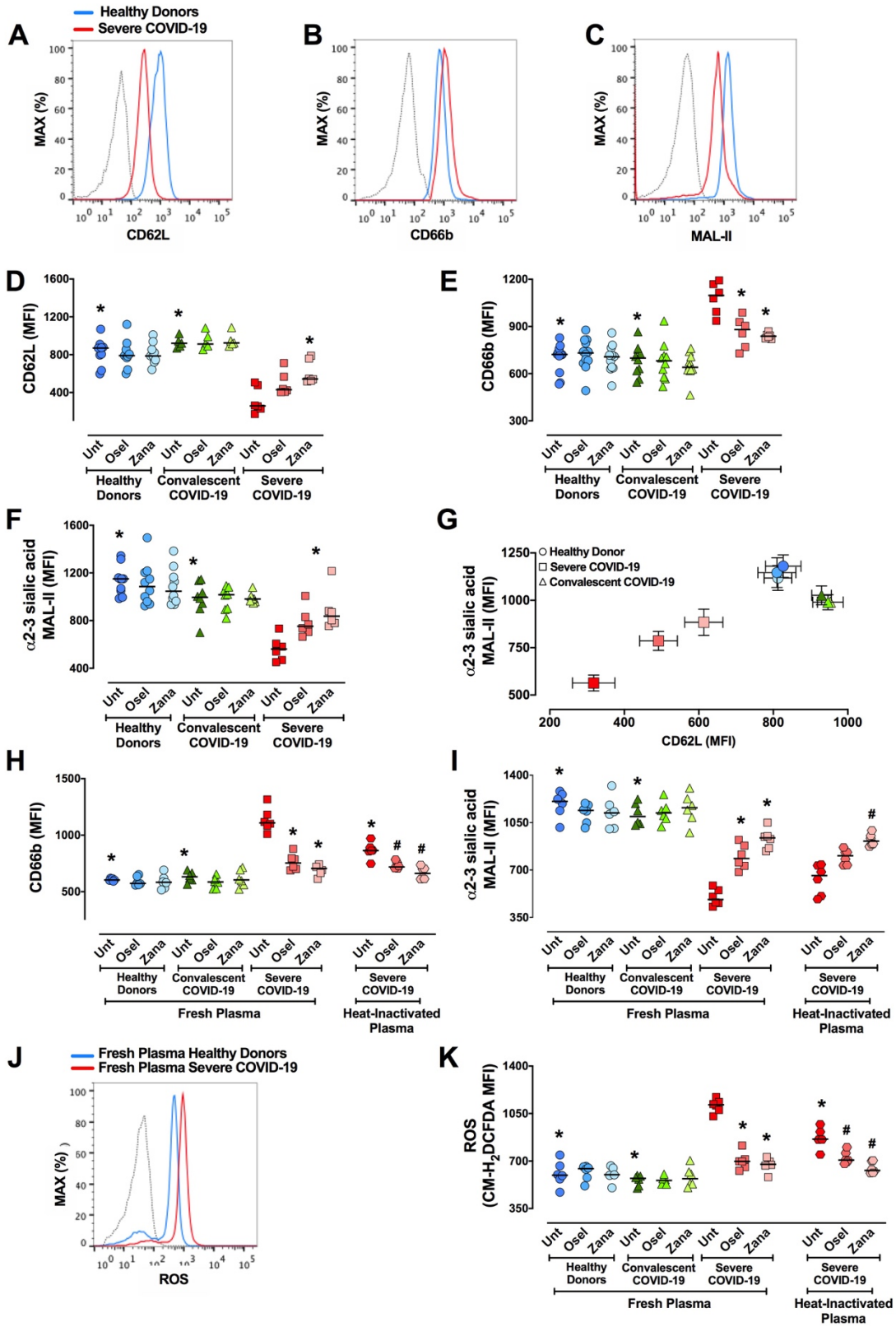


**Figure 6. Oseltamivir and Zanamivir decrease neutrophil activation and increase α2-3 sialic acid levels in active, but not convalescent neutrophils from COVID-19**

904 **patients.** Whole blood from healthy donors (n= 10), severe COVID-19 patients (n= 6) and
905 convalescent COVID-19 patients (n= 8) were treated or not with Oseltamivir (100 μM) or
906 Zanamivir (30 μM) and total leukocytes were stained with the cell activation markers
907 CD62L (**A and D**), CD66b (**B and E**) and MAL-II to detect α2-3 sialic acids (**C and F**).
908 Correlation of surface levels of α2-3 sialic acids vs CD62L (**G**). Blood samples from
909 healthy donors (n = 7) were incubated for 2 h (37 °C, 5% $CO_2$) with 7% of fresh plasma
910 from healthy donors, severe or convalescent COVID-19 patients or with 7% of heat-
911 inactivated plasma from severe COVID-19 patients in the presence or absence of
912 Oseltamivir (100 μM) or Zanamivir (30 μM) and levels of CD66b (**H**), surface α2-3-Sia
913 (MAL-II) (**I**), and ROS production (**J, K**) were assessed by FACS. The MFI was analyzed
914 on $CD66b^+$ cells using the gate strategies shown in Supplementary Fig. 1. Symbols
915 represent individual donors and data are shown as scatter dot plot with line at median
916 from pooled data of two to seven independent experiments. The statistical significance
917 between the groups was assessed by ANOVA followed by a multiple comparisons test of
918 Tukey. The accepted level of significance for the test was $P<0.05$. * was significantly
919 different when compared with Untreated Severe COVID-19; # was significantly different
920 when compared with Untreated Heat-Inactivated Plasma from Severe COVID-19. Osel =
921 Oseltamivir; Zana = Zanamivir.
922

## Supplementary Data

## Supplementary Figures and Figure Legends

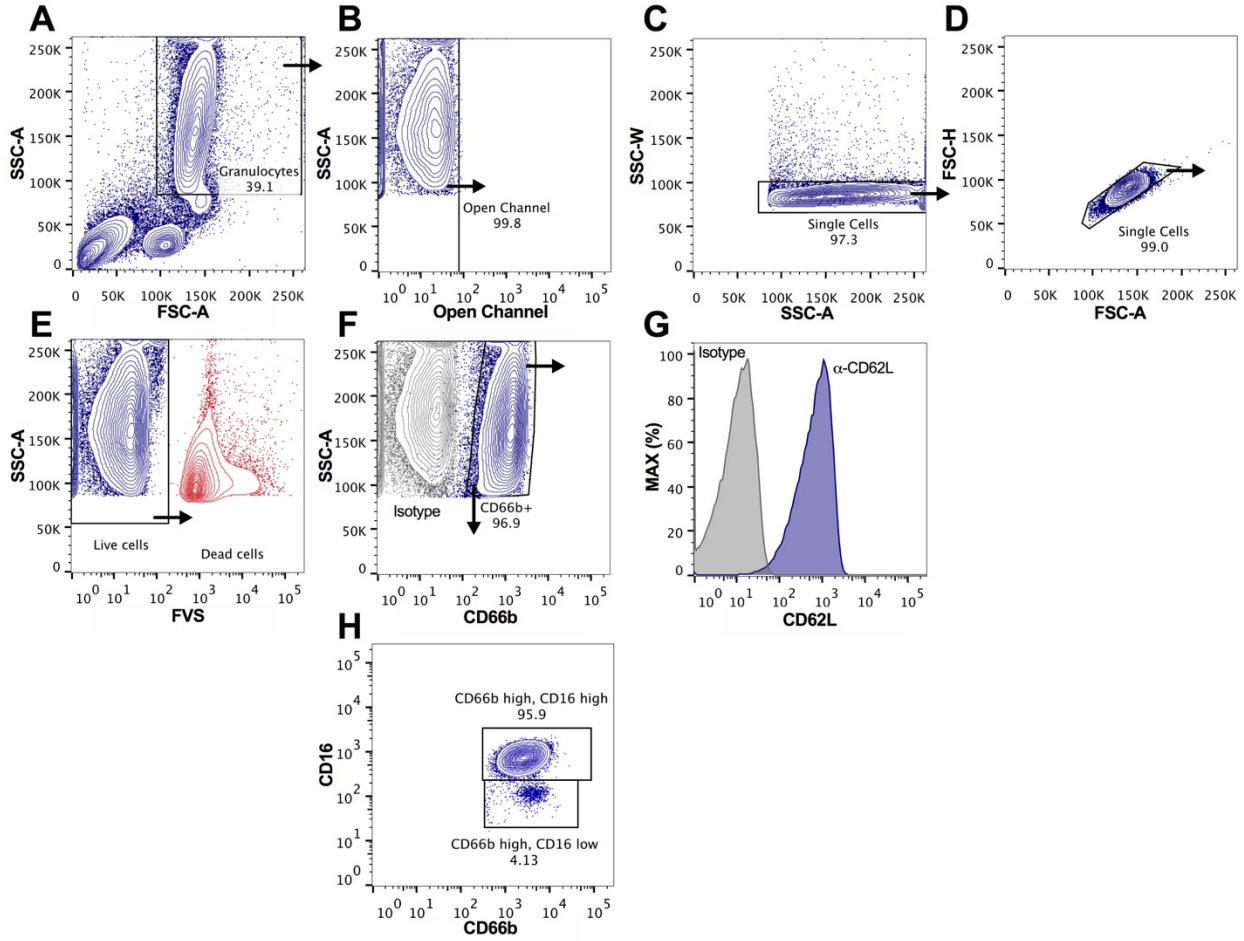


**Supplementary Fig. 1. Representative gate strategy used for neutrophils analysis.** A classic forward-scatter (FSC) vs side-scatter (SSC) characteristic dot plot was used to select neutrophils population (**A**) from peripheral blood collected from healthy donors and patients. Autofluorescent (**B**) and doublets (**C-D**) were excluded and live cells were selected (**E**). CD66b$^{+}$ positive cells (**F**) were gated and the MFI of surface markers, such as CD62L (**G**) were assessed. Around 96% of CD66b$^{+}$ cells are mature neutrophils (CD66b-high/CD16-high) and 4% of CD66b$^{+}$ cells are CD66b-high/CD16-low, which is suggestive of immature neutrophils or eosinophils (**H**). Approximately 100.000 gated events were collected in each analysis. The analysis was performed in a FACSVerse using FACSuite software (BD Biosciences) and FlowJo software (FlowJo LLC).

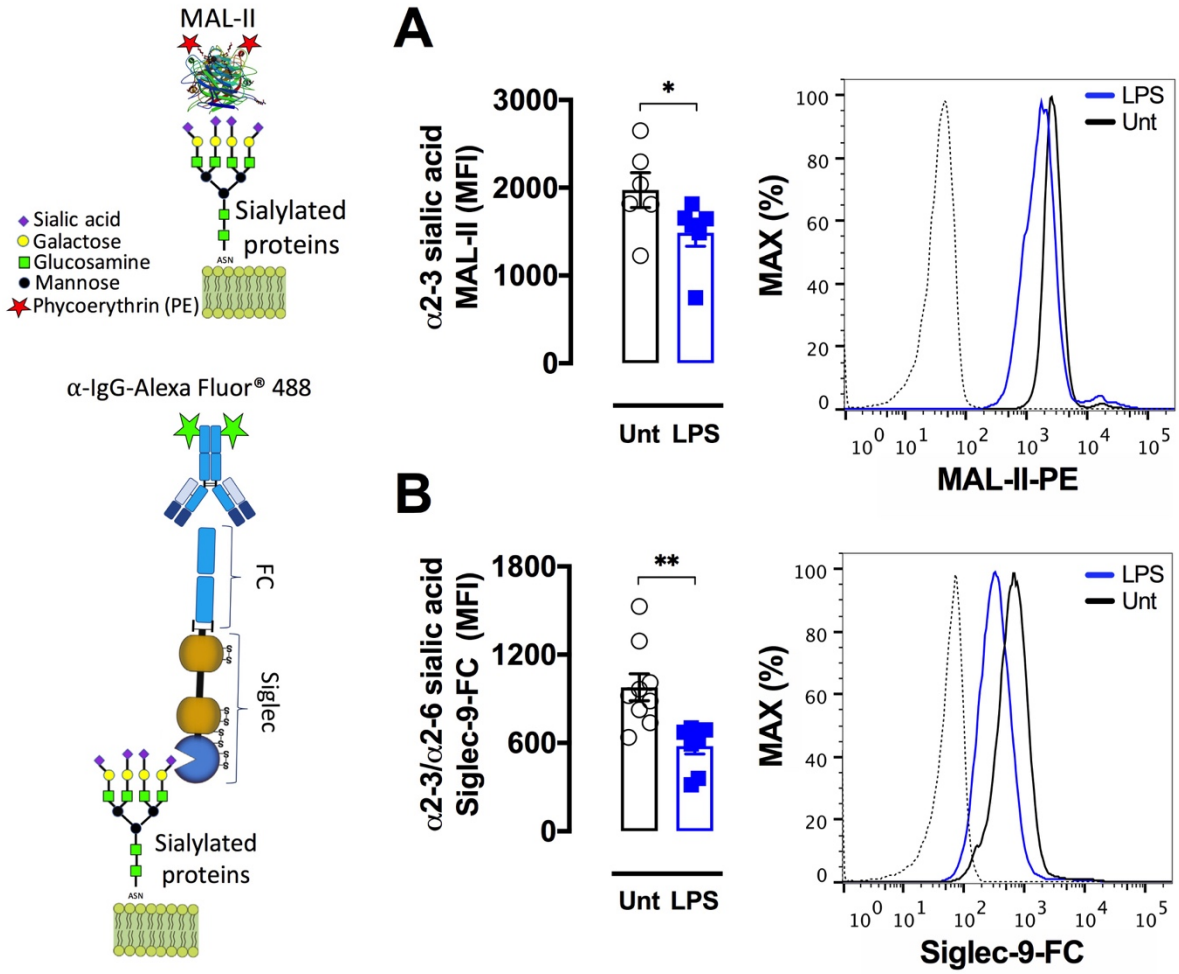


**Supplementary Fig. 2. LPS reduces surface α2-3 sialic acids from human neutrophils**. Whole blood containing 1 x $10^6$ leukocytes from healthy donors were stimulated with 1 µg/mL LPS for 90 min and α2-3 sialic acid contents were assessed by staining cells with biotinylated *Maackia Amurensis* Lectin II (MAL-II) (**A**) followed by streptavidin-phycoerythrin (PE) incubation. Siglec-9 ligands (**B**) were labeled by incubation of chimeric protein containing Siglec-9 sialic acid-Ig binding domain fused to a human IgG-Fc portion (Siglec-9-Fc). Siglec-Fc-9 were incubated with α-IgG1-Alexa Fluor 488 before adding the probe to cells. The MFI was analyzed on CD66b$^+$ cells using the gate strategies shown in Supplementary Fig. 1. *$P$ < 0.05. Symbols represent individual donors and data are shown as mean ± SEM from pooled data of two to three independent experiments (n=6-9). Unt = untreated cells; LPS = lipopolysaccharide; dotted line = unstained cells.

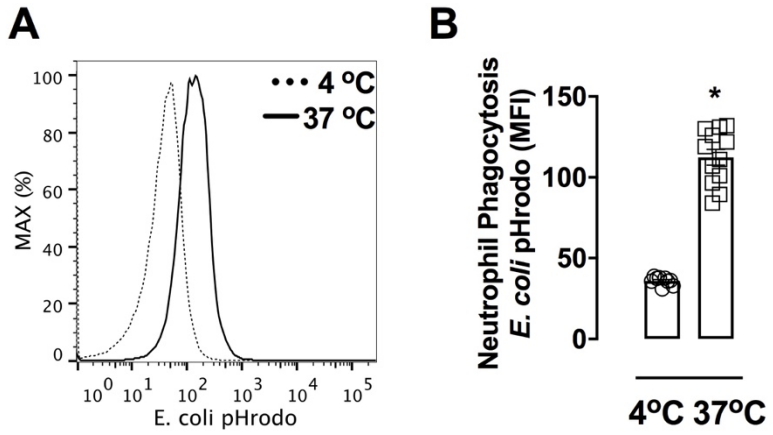


**Supplementary Fig. 3. Phagocytosis of *E. coli* pHrodo bioparticles at 4 °C and 37 °C.** Total leukocytes (1 x$10^6$) were incubated with *E. coli* pHrodo bioparticles (100 µg/mL) for 60 min at 4°C or 37 °C and the phagocytosis in viable CD66b$^+$ cells was assessed. Symbols represent individual donors and data are shown as mean ± SEM from pooled data of three to four independent experiments (n = 9-12). *$P$ < 0.001.

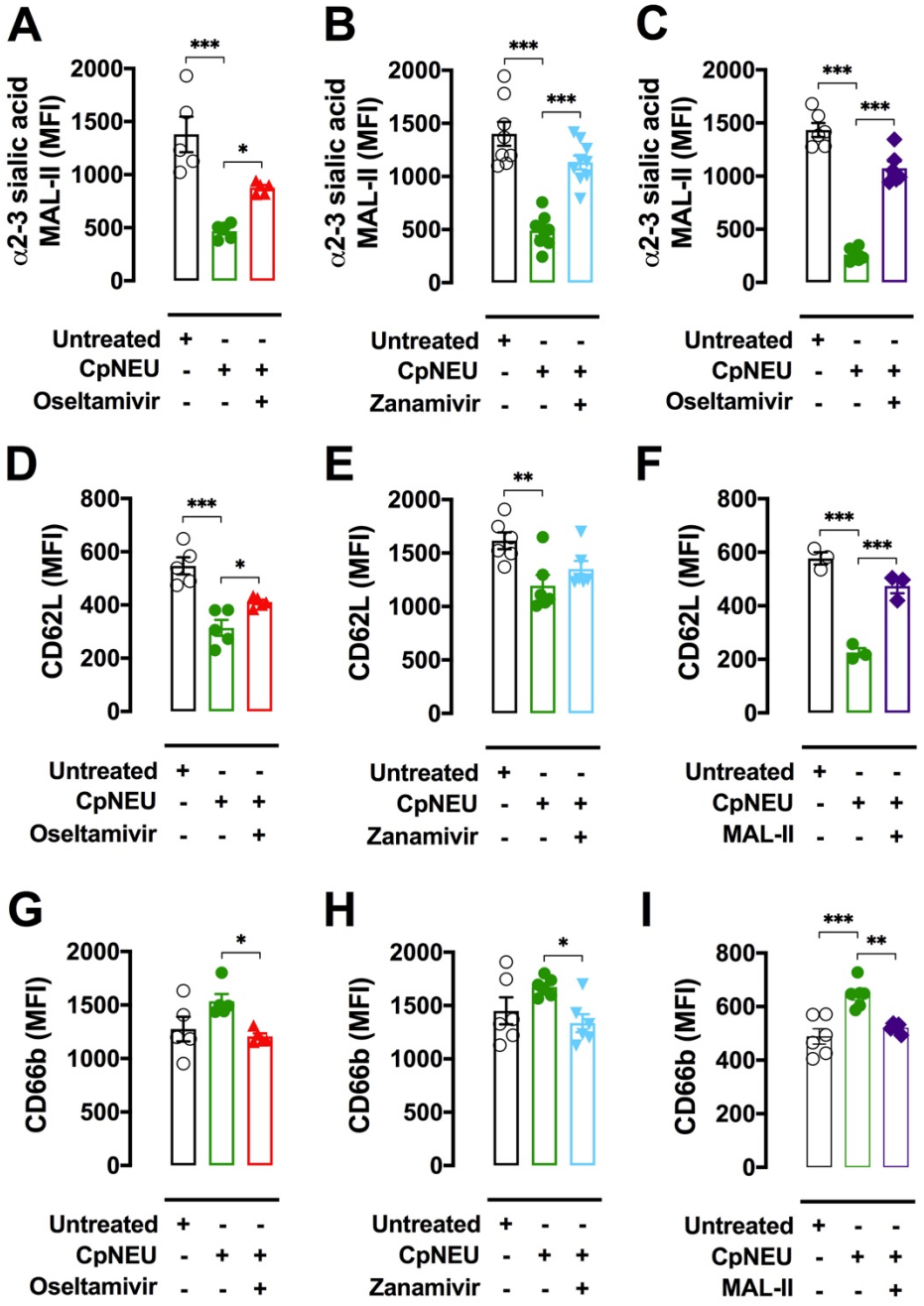


959

960 **Supplementary Fig. 4. CpNeu-induced human neutrophil activation.** Total
961 leukocytes (1 x $10^6$) were incubated or not with CpNEU (10 mU, 60 min, 37 $^oC$, 5%
962 $CO_2$) CpNEU plus Oseltamivir (100 μM), CpNEU plus Zanamivir (30 μM) or CpNEU plus
963 MAL-II (1 μg/mL). Leukocytes were stained with MAL-II to detect α2-3 sialic acids (**A-C**)
964 or with cell activation markers CD62L (**D-F**) and CD66b (**G-I**). The MFI was analyzed on
965 $CD66b^+$ cells. Symbols represent individual donors and data are shown as mean ± SEM

966 from pooled data of two to three independent experiments (n = 5-9) except for F that
967 was made once with n=3. *$P < 0.05$; **$P < 0.01$; ***$P < 0.001$. MAL-II = *Maackia*
968 *amurensis* lectin II; CpNEU = neuraminidase *Clostridium perfringens*.
969

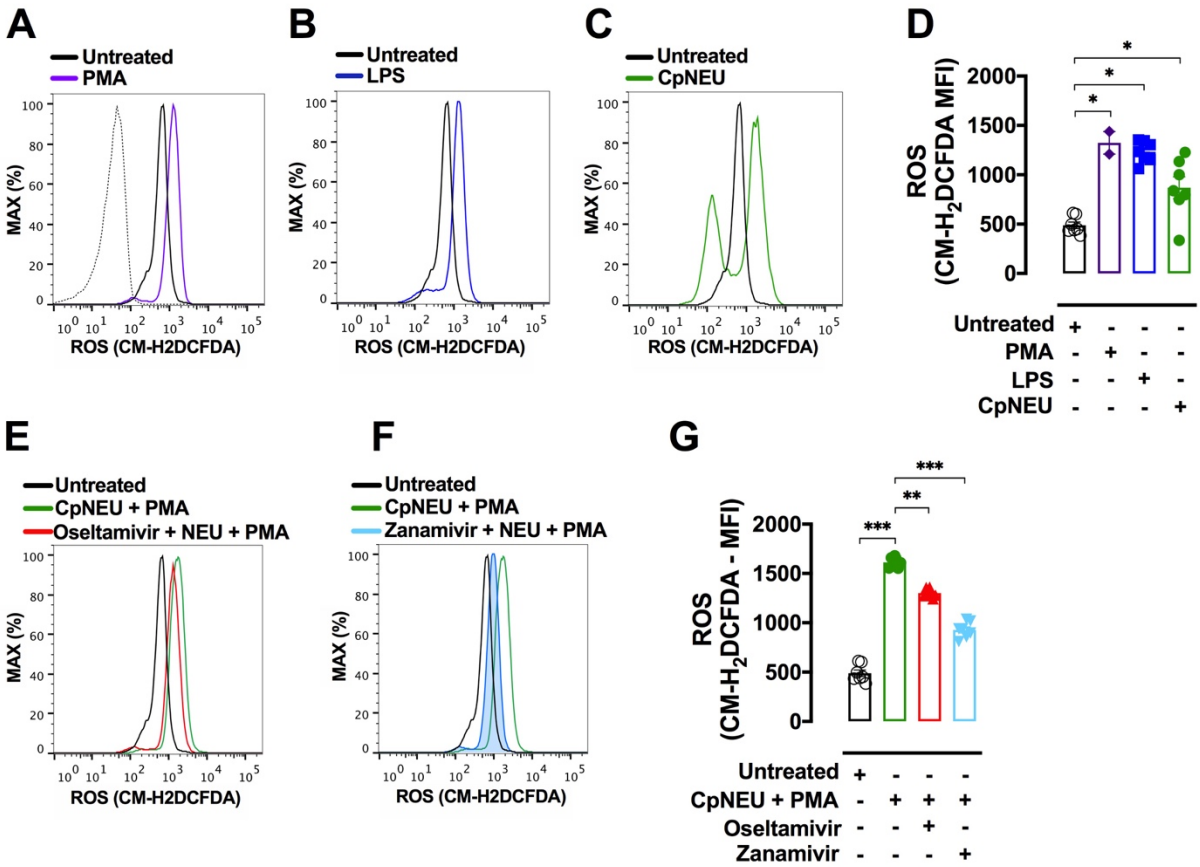


**Supplementary Fig. 5. ROS production in neutrophils stimulated with LPS, CpNEU, or PMA.** Whole blood from healthy donors containing 1 x $10^6$ leukocytes were exposed or not to LPS (1 µg/mL, 90 min) (**B and D**). Total leukocytes (1 x $10^6$) were incubated or not with CpNEU (10 mU, 60 min) (**C-D**), CpNEU plus Oseltamivir (100 µM) or CpNEU plus Zanamivir (30 µM) (**E-G**). Leukocytes were incubated with 5 µM CM-H2DCFDA fluorescent probe for 15 min and PMA (10 µM) was used to stimulate ROS production for 10 min (**A and E-G**). The MFI was analyzed on CD66b$^+$ cells**.** Symbols represent individual donors and data are shown as mean ± SEM from pooled data of two independent experiments (n = 2-6). *$P < 0.05$; **$P < 0.01$; ***$P < 0.001$. C = control; CM-H2DCFDA = 5-(and-6)-chloromethyl-2',7'-dichlorodihydrofluorescein diacetate, acetyl ester; LPS = lipopolysaccharide; CpNEU = neuraminidase *Clostridium perfringens*; PMA = phorbol 12-myristate 13-acetate.

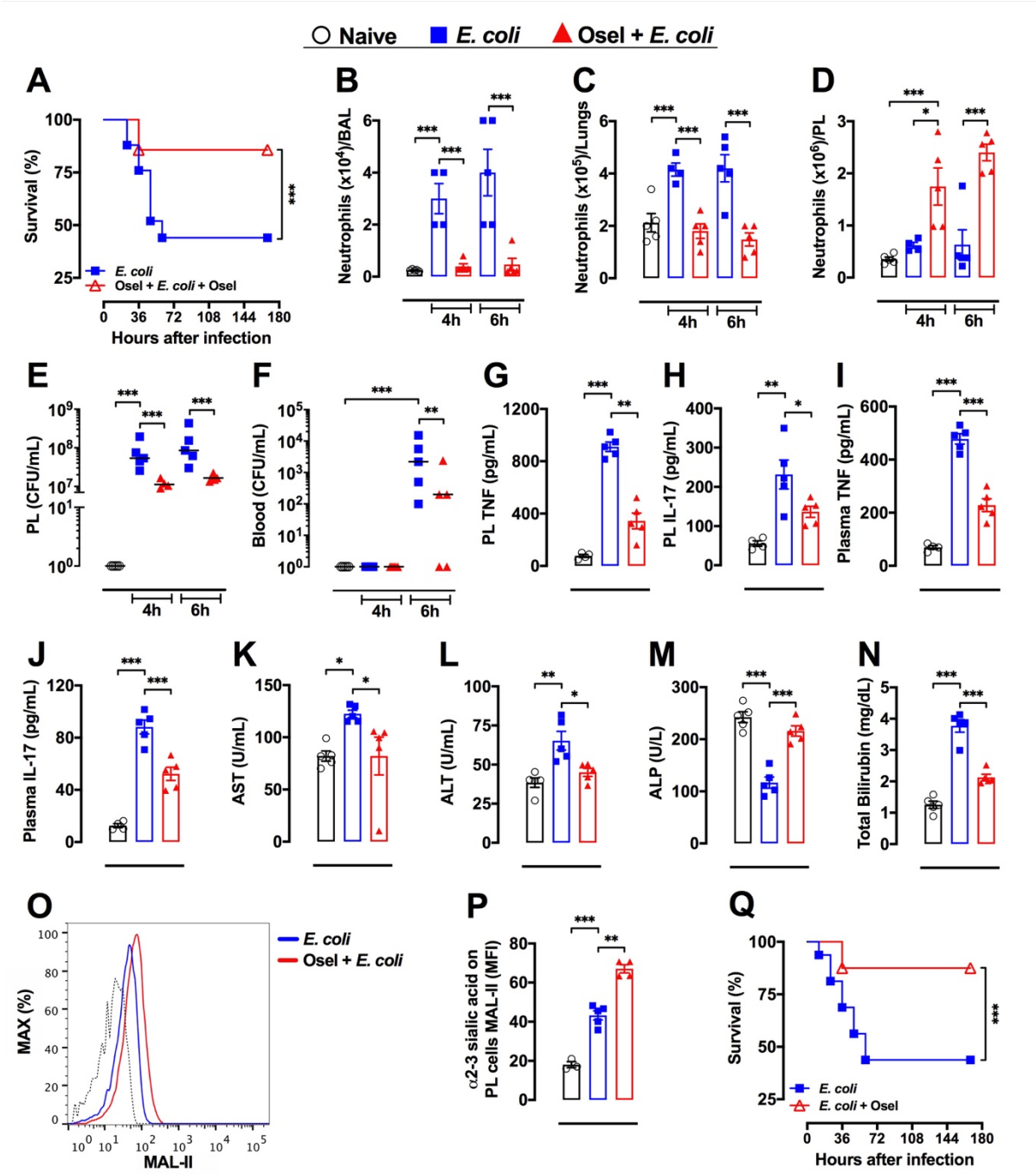


**Supplementary Fig. 6. Oseltamivir improved the outcome of *E. coli*-induced sepsis.** Sepsis was induced by intraperitoneal (IP) administration of 1 × $10^7$ CFU/mice *E. coli* (ATCC 25922). Mice were randomly pretreated *per oral* (PO) via (2 hr before infection) and posttreated (6 hr after infection, 12/12 hr, PO, for 4 days) with Oseltamivir phosphate (Osel, 10 mg/Kg) or saline and their survival rates were monitored over 168 hr (**A,** n=16). In another set of experiments (n=3-5) mice were randomly pretreated (2 hr

991 before infection) with Oseltamivir phosphate (10 mg/Kg, PO) and the number of
992 neutrophils in bronchoalveolar lavage (BAL, **B**) and in lung tissue (**C**) was counted. In
993 peritoneal lavage (PL) infiltrating neutrophils counts (**D**), TNF (**G**), IL-17 (**H**) and the
994 number of colony-forming units (CFU) in PL (**E**) or blood (**F**) were determined 4 or 6 hr
995 after infection. Plasma levels of TNF (**I**), IL-17 (**J**), AST (**K**), ALT (**L**), ALP (**M**) and total
996 bilirubin (**N**) were evaluated. The amount of surface α2-3 sialic acids were also
997 assessed in PL $SSC^{high}$/Gr-$1^{high}$ cells as shown by the representative histograms (**O**) or
998 MFI (**P**); dotted line = unstained cells. Mice were also randomly posttreated (starting 6
999 hr after infection, 12/12 hr, PO, for 4 days) with saline or Oseltamivir phosphate (10
1000 mg/Kg) and their survival rates were monitored over 168 hr (**Q**). The results are
1001 expressed as percent of survival (n=16), mean or median (only for FACS data) ± SEM.
1002 *$P < 0.05$; **$P < 0.01$; ***$P < 0.001$. These experiments were repeated 3 times for
1003 survival analysis and twice for other parameters. Osel = Oseltamivir; AST = alanine
1004 aminotransferase; ALT = aspartate aminotransferase; ALP = alkaline phosphatase;
1005 MAL-II = *Maackia amurensis* lectin II.

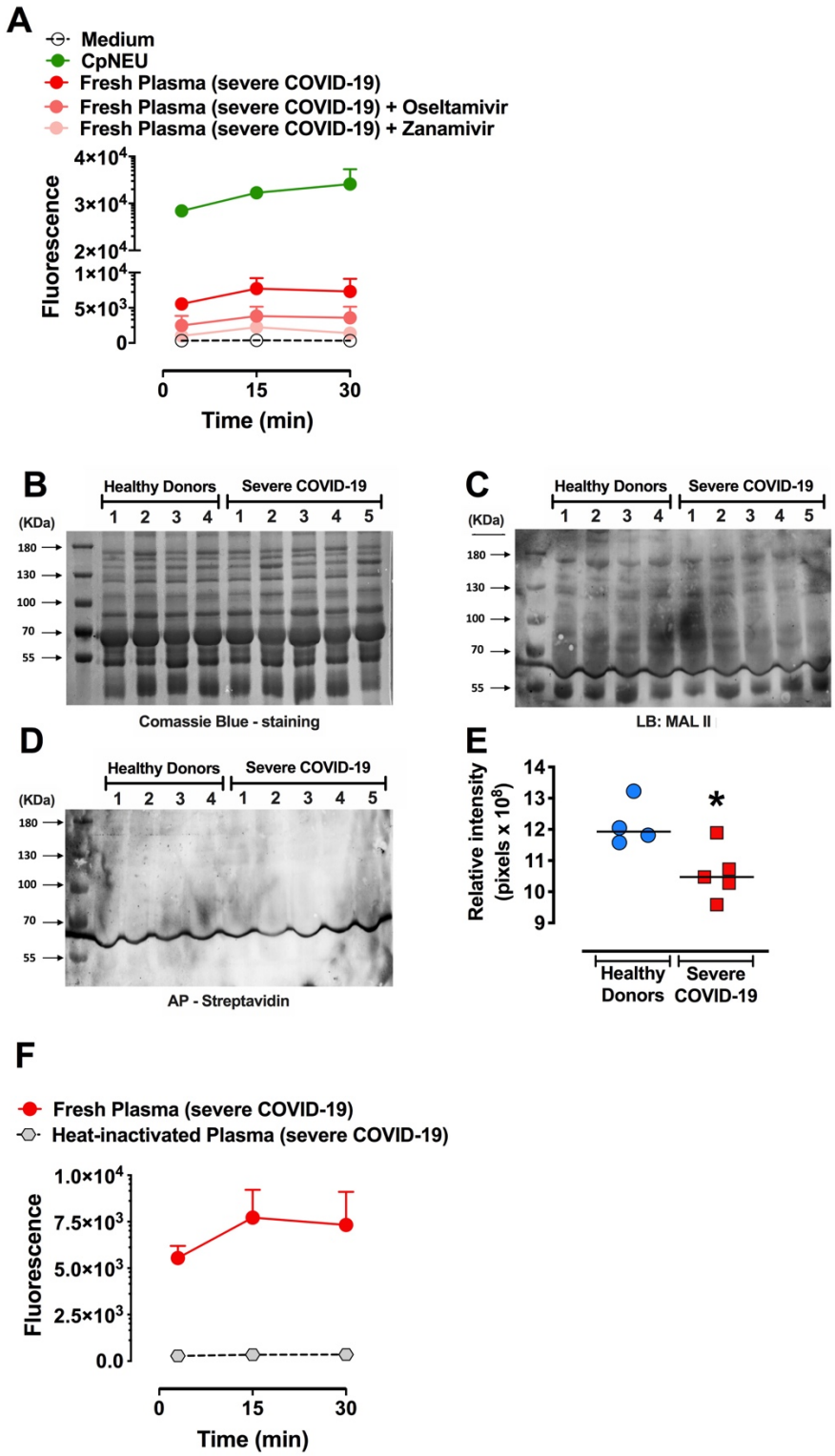


**Supplementary Fig. 7. NEU activity is increased in plasma from severe COVID-19 patients.** NEU activity was evaluated in fresh plasma from severe COVID-19 patients in the presence or absence of Oseltamivir (100 μM) or Zanamivir (30 μM) (**A**) and in heat-

1010 inactivated plasma from COVID-19 patients (**F**). Neuraminidase isolated from
1011 *Clostridium perfringens* (CpNEU) was used to validate the NEU activity assay. Twelve
1012 µg of total serum proteins from healthy donors (n=4) or severe COVID-19 patients (n=5)
1013 were separated by SDS-PAGE 10% and stained with coomassie blue (**B**). Lectin
1014 blotting (LB) were performed with biotin-conjugated MAL-II for staining α2-3 sialic acid-
1015 containing proteins **(C)** or membrane were incubated with AP-Streptavidin without MAL-
1016 II (as a control) **(D).** The intensity of lectin staining of each lane was evaluated and
1017 normalized to the total proteins on corresponding gel lanes **(E)**; *p=0.02 Unpaired t test -
1018 Welch's correction**.** MAL-II = *Maackia amurensis* lectin II; CpNEU = neuraminidase
1019 *Clostridium perfringens*.
1020
1021

1022

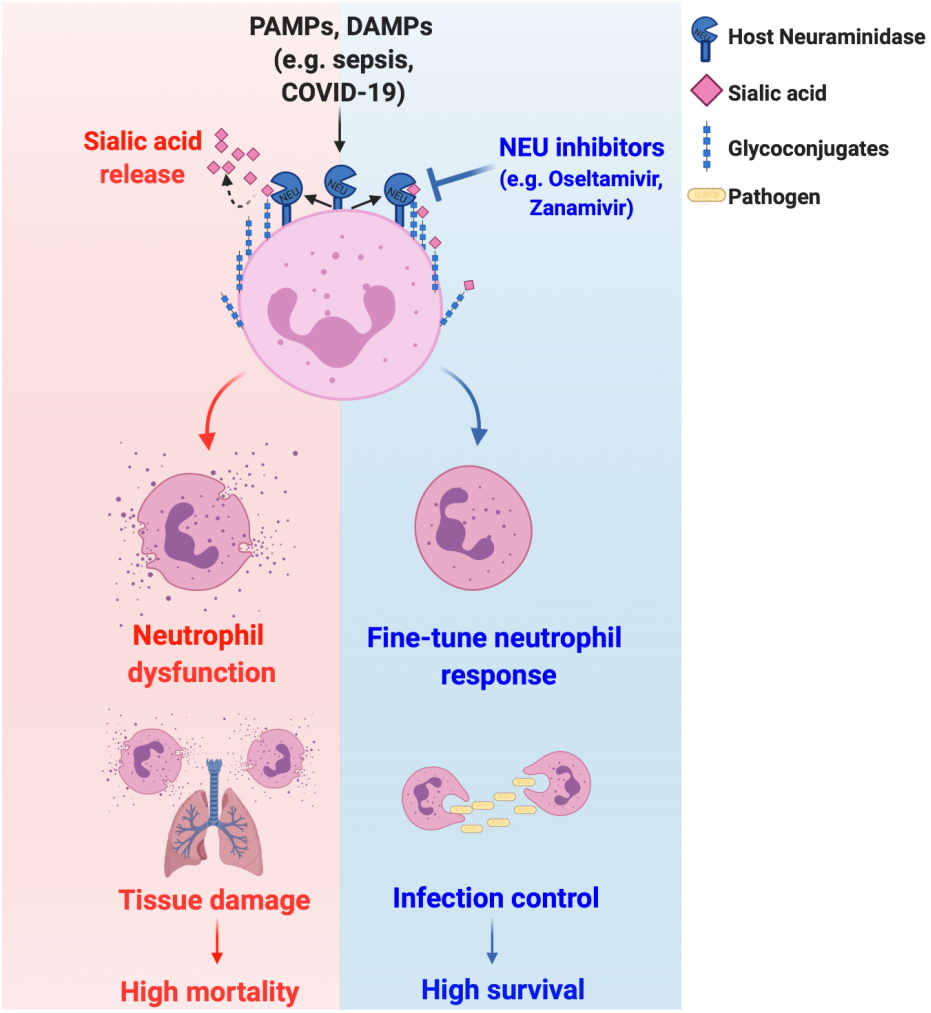


1023
1024
1025 **Supplementary Fig. 8. Working model.** PAMPs and DAMPs in severe diseases such
1026 as sepsis and COVID-19 lead to neuraminidase activation with shedding of surface
1027 sialic acid and neutrophil overactivation, resulting in tissue damage and high mortality
1028 rates. On the other hand, neuraminidase inhibitors (e.g., Oseltamivir, Zanamivir) prevent
1029 the sialic acid release to regulates neutrophil response, resulting in infection control and
1030 high survival rates.
1031

1032 **Supplementary Table 1.**

1033

1034 **Supplementary Table 1. Clinical information of samples from UFSC University**
1035 **Hospital, SC, Brazil**

1036

| | ***Severe COVID-19*** | ***Convalescent COVID-19*** |
|---|---|---|
| ***Characteristic*** | | |
| Gender (Male/Female) | 3/2 | 7/5 |
| Age (years) | 44.4 (25;65) | 53.2 (36;80) |
| Weight (kilos) | 90.0 (62.2;127) | 85.1 (51.8;150) |
| Height (m) | 1.72 (1.65;1.8) | 1.7 (1.55;1.83) |
| Cough | 4 (80%) | 8 (66.7%) |
| Dyspnea | 4 (80%) | 5 (41.7%) |
| Chest Pain / Oppression | 1 (20%) | 4 (33.3%) |
| Asthenia | 2 (40%) | 3 (16.7%) |
| Myalgia | 3 (60%) | 3 (16.7%) |
| Anosmia | 1 (20%) | 5 (41.7%) |
| Ageusia / Dysgeusia | 1 (20%) | 4 (33.3%) |
| Fever | 3 (60%) | 3 (16.7%) |

| | | |
|---|---|---|
| Paresthesia | 0 (0%) | 0 (0%) |
| Headache | 0 (0%) | 2 (16.7%) |
| Diarrhea | 0 (0%) | 1 (8.3%) |
| Diabetes mellitus | 3 (60%) | 4 (33.3%) |
| Systolic BP (mmHg) | 132.2 (100;150) | 126.4 (100;177) |
| Diastolic BP (mmHg) | 84.2 (80;90 | 78.55 (60;102) |
| Heart rate (bpm) | 96.4 (80;115) | 86.4 (72;115) |
| Respiratory frequency (bpm) | 20.8 (18;25) | 20.8 (11;29) |
| Length of hospitalization (days) | 6.6 (4;10) | 8.3 (3;16) |
| Mechanical ventilation | 0 (0%) | 3 (16.7%) |
| Mechanical ventilation time (days) | 0 (0%) | 7.3 (5;9) |
| Saturation (O2%) | 90.4 (85;97) | 93.3 (86;99) |
| SOFA Score | 0.17 (0;1) | 0.6 (0;2) |
| ***Laboratory data*** | | |
| Hemoglobin (g/dL) | 13.5 (11;15) | 13.65 (11.3;15.7) |
| Hematocrit (%) | 40 (33.4;47.1) | 40.2 (34.8;45.5) |

| | | |
|---|---|---|
| Leukocytes (/μL) | 7988 (4070;12930) | 8098 (5330;10660) |
| Neutrophils (/μL) | 5731 (3355;10098) | 6448.5 (3923;9135) |
| Lymphocytes (/μL) | 1526 (451;3728) | 955.8 (208;1687) |
| Monocytes (/μL) | 369 (253;483) | 473.2 (168;961) |
| Platelets ($x10^3$/μL) | 235 (115:314) | 238 (117;436) |
| PCR (mg / dL) | 52.5 (22;78.7) | 90.7 (15;214) |

1040 **Supplementary Table 2. Clinical information of**
1041 **samples from Hospital Naval Marcílio Dias, RJ,**
1042 **Brazil**

| *Characteristic* | *Severe COVID-19* |
|---|---|
| Gender (Male/Female) | 2/3 |
| Age (years) | 66 (55-73) |
| Cough | 4 (80%) |
| Dyspnea | 4 (80%) |
| Chest Pain / Oppression | 0 (0%) |
| Asthenia | 1 (20%) |
| Myalgia | 2 (40%) |
| Anosmia | 2 (40%) |
| Ageusia / Dysgeusia | 0 (0%) |
| Fever | 4 (80%) |
| Paresthesia | 0 (0%) |
| Headache | 0 (0%) |
| Diarrhea | 3 (60%) |

| | |
|---|---|
| Diabetes mellitus | 3 (60%) |
| Systolic BP (mmHg) | 141.4 (108;166) |
| Diastolic BP (mmHg) | 74.8 (51;100) |
| Heart rate (bpm) | 83.8 (57;102) |
| Respiratory frequency (bpm) | 24 (14-40) |
| Length of hospitalization (days) | 32.8 (10;90) |
| Mechanical ventilation | 5 (100%) |
| Saturation (O2%) | 87.3 (83;91) |

| ***Laboratory data*** | |
|---|---|
| Hemoglobin (g/dL) | 11.92 (7.9;13.3) |
| Hematocrit (%) | 35.72 (23;41.6) |
| Leukocytes (/μL) | 7900 (5400;12100) |
| Neutrophils (/μL) | 5724.8 (4266;7502) |

| | |
|---|---|
| Lymphocytes (/μL) | 983.8<br>(430;1694) |
| Monocytes (/μL) | 575.8<br>(216;1452) |
| Platelets (x$10^3$/μL) | 172.8<br>(109;219) |
| PCR (mg / dL) | 15.8<br>(5.16;26.8) |

1043
1044